1964

The mechanics of column deflection curves, June 1964

M. G. Lay

Welded Continuous Frames and Their Components

THE MECHANICS OF COLUMN DEFLECTION CURVES

By

M. G. Lay

This work has been carried out as part of an investigation sponsored jointly by the Welding Research Council and the Department of the Navy with funds furnished by the following:

American Institute of Steel Construction
American Iron and Steel Institute
Institute of Research, Lehigh University
Column Research Council (Advisory)
Office of Naval Research (Contract No. 610 (13))
Bureau of Ships
Bureau of Yards and Docks

June 1964

Fritz Engineering Laboratory
Department of Civil Engineering
Lehigh University
Bethlehem, Pennsylvania

Fritz Engineering Laboratory Report No. 278.12

TABLE OF CONTENTS

I. INTRODUCTION

a) Statement of Problem

This report will discuss the behavior of structural members subjected to planar loading. A structural member is defined as a component in which one dimension (length) is significantly greater than the other two (width and depth). It will be assumed that the members are bi-symmetric and are loaded in a principal plane. Consequently the deformations will be confined to the same plane as the loads. It will be further assumed that the members under consideration are only loaded at their ends.

Such a member is shown in Fig. 1a. It is subjected to an axial load P (positive in compression), end-moments M_L and M_R (of the same sign when they cause curvatures of the same sign) and shears V (positive when they cause a clockwise couple). The undeformed length of the member is ℓ.

If equilibrium is formulated on the undeformed structure, then

$$V = \frac{M_R - M_L}{\ell} \tag{1}$$

The positive direction of the moments is such that the moment assigned to the left hand position is positive when clockwise.

These forces and moments may be combined into a single force which is generally not coincident with the centroid of the member. This compounded force F is shown in Fig. 1b. The position of F is defined by ω, its counterclockwise rotation from LR, and ηL, the distance from its intersection with LR to L measured in the LR direction. The values of ω, η and F are

$$\tau = \arctan \frac{M_R - M_L}{P\ell} \tag{2}$$

$$\eta = \frac{M_L}{M_R - M_L} \tag{3}$$

and

$$F = P \sec \tau \tag{4}$$

b) Analysis

In the remainder of this report the effects of deformations due to shear will be neglected and it will be assumed the internal resisting moment of a cross-section, M_i can be expressed as a function of the curvature at the centerline*, ϕ, i.e.

$$M_i = M_i(\phi) \tag{5}$$

For a material such as structural steel, eq.(5) will be non-linear and history-dependent over much of its range.

The deformed shape of the member previously discussed in Fig. 1a is shown in Fig. 2a. The length ℓ^* is the chord length and is ℓ reduced by the effect of axial deformation and curvature shortening. The equilibrium of any point on the member is expressed by the equation

$$Pv + M_L + (M_R - M_L)\frac{w}{\ell^*} = M_i(\phi) \tag{6}$$

where w and v are co-ordinate axes along, and normal to, the chord of the member. If $(dv/dw)^2$ is small with respect to unity then eq.(6) can be written as

$$Pv + M_L + (M_R - M_L)\frac{w}{\ell^*} = M_i\left(\frac{d^2v}{dw^2}\right) \tag{7}$$

The solution of this differential equation gives the deformed shape of the member. As M_i is both non-linear and history-dependent this solution will

---

* The centerline curvature is specified in order to eliminate any ambiguities in the inelastic range.

not generally be unique.

c) Column Deflection Curves

Solutions of eq.(7) for materials which are not perfectly elastic must usually be obtained numerically. Hence the solution of each structural problem involving a non-elastic member is both involved and tedious. A considerable simplication is achieved by using the system shown in Fig. 1b. The deformed shape for this system is shown in Fig. 2b.

The equilibrium equation is now

$$Fy = M_i(-y'') \tag{8}$$

where y is the deflection of the member from the F axis and y" is the second derivative with respect to the co-ordinate, x, along this axis. Relative to eq.(7), eq.(8) only represents a simple shift of co-ordinate axes and in itself is not a significant simplification. However there is no reason why the calculations need be stopped at the ends, L & R, of the member. If the calculations are allowed to continue a wave-like function (shown dashed in Fig. 2b) will be obtained. Clearly, just as the portion LR of the function represents the deformed shape of a member, so some other portion represents the deformed shape of another member. The function generated by solving the particular case of member LR therefore also represents an accessible source of information with regard to numerous other loading configurations.

d) Historical Review

Continuous solutions to eq. (8) provide the functions shown in

Fig. 2b. In the elastic range these solutions are the characteristic functions (or eigenvectors) of eq.(8) and are therefore derived directly from the classical Euler solution.

In the post-elastic range, the moment and curvature are not linearly related and a closed solution to eq.(8) is not possible in many cases. In 1910 von Karman[1] used numerical double integration techniques to handle the non-linear moment-curvature relations and applied the method to predict the behavior of columns with small eccentricities of axial load. Von Karman's solution[1] forms the basis for much subsequent work, however it is noted that his particular solution is for the beam-column case of Figs. 1a and 2a and that he considered only relatively small end-moments.

Von Karman's work was generalized by Chwalla[2] in 1934. Chwalla solved the problem of Fig. 1b and 2b and called the continuous functions which he derived "grundkurven" (basic curves). Today the curves are more widely known as "column deflection curves." Chwalla's development in Ref.2 must be regarded as the foundation and forerunner of all present column deflection curve developments.

The curves were derived for rectangular sections, however their scope was widened when, in 1935, Chwalla published[3] similar curves for a variety of shapes, including the I section.

A third publication[4] by Chwalla (1937) is of considerable importance as it shows how the column deflection curve approach may be applied to continuous columns and thus to columns which are intergral parts of a structure.

Surprisingly, little further was done to advance the method until about 20 years later. In 1958, Ellis[5] used the column deflection

curve approach for annular sections and also contrubuted a method for quickly determining the maximum end-moment that a beam-column can carry. However Ellis was apparently unaware of Chwalla's earlier derivations.[2,3,4] Ojalvo[6] in 1960 adopted Chwalla's work and recomputed the curves for the moment-curvature relations relevant to U.S. wideflange sections. In addition, Ojalvo[6] contributed techniques which allowed the column deflection curve data to be presented in a much more accessible form, and elaborated on their use in the analysis of beam-columns which are parts of continuous structures.

Finally, Neal and Mansell[7] have applied the column deflection curve method to truss analysis. In thus treating a small eccentricity problem, it is interesting to note that the theory has come a full cycle since von Karman's original development.

The beam-column problem has also been attacked from a number of different aspects. The fact that Chwalla's results had to be presented in graphical or tabular form caused a number of investigators to look for closed solutions.

A popular[8,9] technique was a form of the collocation method in which a function was assumed to represent the deformed shape of the member. The unknowns in the assumed function were found by satisfying eq.(8) at a sufficient number of discrete points. The advent of high speed computation has now removed the algebraic attractiveness of the above method.

Bijlaard's work[9b] is of additional interest as it also contains an extension of the column deflection curve system outlined by Chwalla,[4]

and thus represent the first major appreciation of this system.

A more exact approach is due to Horne,[10] who used eq.(8) in its integral form (see Section II). For a number of elementary situations, such as the rectangle with a trapezoidal stress-strain diagram, closed solutions can be obtained. However the number of such situations is very restricted and for the more realistic cases it is again necessary to use numerical integration. When closed solutions are possible, a different function will be obtained for each yielded configuration of the member, with the subsequent necessity of matching various boundary conditions.

Horne's method[10] forms the basis for the Cambridge approach to predicting the behavior of beam-columns in plastically designed structures. The results are presented in the form of beam-column data, however it may be noted that the method of presentation is close to the column deflection curve system. With only minor extensions and changes in parameters the Cambridge results could be changed to the more general column deflection curve representations, with a considerable increase in their range of applicability.

The remainder of this report will discuss the column deflection curve method of Chwalla[2,3,4] using both the numerical[6] and the closed[10] solutions to eq.(8). The collocation method will not be discussed further.

II ALBEBRAIC PROPERTIES OF COLUMN DEFLECTION CURVES

a) Form of the Curves

The form of the column deflection curves(CDC's) may be studied by examining a partial solution to eq.(8), in a manner suggested by Mansell.[11] Defining

$$\theta = y' \tag{9}$$

gives

$$\theta d\theta = y'' dy = -\phi dy \tag{10}$$

where

$$\phi = -y'' \tag{11}$$

Integrating eq.(10)

$$\tfrac{1}{2}\theta^2 \Big| = -\int \phi dy \tag{12}$$

Taking the x axes at y=o and the slope there as θ_0 (Fig. 2b) gives

$$\theta^2 = \theta_0^2 - 2\int_0^y \phi dy \tag{13}$$

From eq.(8)

$$dy = \frac{1}{F} dM \tag{14}$$

and so eq.(13) becomes

$$\theta^2 = \theta_0^2 - \frac{2}{F}\int_0^M \phi dM \tag{15}$$

As Mansell[11] pointed out, eq.(15) will represent a symmetrical periodic function if the M-Ø relationship is odd, of positive slope and single-valued. The first two of these conditions are fulfilled in structural engineering situations, however the third condition applies only to elastic members or to members being loaded into the non-elastic region for the first time. For such members the CDC's will therefore be symmetrical periodic functions and this will be the customary assumption in the remainder of this report. However the problem of inelastic unloading (during which the M-Ø relationship is not single-valued) will be

discussed at length in Section IV.

The equation representing the CDC's can be obtained by integrating eq.(15). As the integral is definite the only constant appearing in the final equation is θ_o, the angle between the CDC and the F-axis. This constant serves to define the CDC's for a particular value of F, and can vary from 0 to $\pi/2$. Its appearance in eq.(15) makes it a natural parameter to use and experience indicates that it is also a very convenient parameter.

b) Calculation of Curves

The solution of eq.(8) for non-linear M-Ø relationships is readily and rapidly achieved by means of numerical integration performed by high speed computers. Such curves are now available in published form.[5,7,12]

One deficiency of these methods is that, being numerical rather than algebraic, they do not allow the influence of various parameters to be studied directly. With the number of variables occurring in column studies it is advantageous to have a method which will allow the significance of the various parameters involved to be studied

Horne's closed solutions[10] were based on a further integration of eq.(15), and a more recent paper[13] by Hauk and Lee has elaborated on, but not simplified, Horne's work. As these methods use a piecewise moment-curvature function the resulting solutions do not have the algebraic simplicity necessary to allow an investigation of the influence of the papameters involved. It might also be noted that the work of Hauk and Lee[13] seems to represent an unnecessary sacrifice of numerical accuracy.[14]

The following section will present an algebraic solution to the

CDC problem based on a simplified continuous representation of the moment-curvature relationship.

c) Moment - Curvature Representation

It is possible to rearrange eq.(15) to give

$$\theta = \frac{dy}{dx} = \sqrt{\theta_0^2 - \frac{2}{F}\int_0^M \phi\, dM} \tag{16}$$

Using eq.(14) and integrating gives

$$x = \frac{1}{F}\int_0^M \frac{dM}{\sqrt{\theta_0^2 - \frac{2}{F}\int_0^M \phi\, dM}} \tag{17}$$

This equation is the solution in integral form of eq.(8), and is the equation of the CDC's. It is the basis of Horne's[10] original closed solution.

This CDC equation has very few solutions. The difficulty can be seen if it is realized that the relation between ϕ and M must be such that the interior integral in eq.(17) must give solutions which allow the major integral to be solved. This restricts the M-ϕ relation to very simple functions. On the other hand the relation must, for physical reasons, be of the form shown in Fig. 3 with an asymptotic approach to the maximum section moment, M_{pc}, as ϕ approaches infinity. The slope must always be positive.

Very few equations satisfy both these requirements. The equation used in this report is

$$\frac{M}{M_{pc}} = 1 - \frac{1}{(1+\phi/N\phi_{pc})^2} \tag{18}$$

where M_{pc} is the plastic moment reduced by axial load, and ϕ_{pc} is the elastic curvature corresponding to this moment. Equation (18) is plotted in Fig. 4. It is seen that the constant N allows the equation to be brought into some degree of approximation to real moment-curvature relations. For instance, it might be suggested that the following approximation holds

$$N = 2 - F/F_y \tag{19}$$

where

$$F_y = A\sigma_y \tag{20}$$

where A is the cross-sectional area and σ_y the yield stress of the material.

The following non-dimensional parameters will be used in the subsequent derivations,

$$m = M/M_{PC} \tag{21}$$

$$\psi = \phi/\phi_{PC} \tag{22}$$

$$n = F/F_y \tag{23}$$

where

$$M_{PC} = EI\,\phi_{PC} \tag{24}$$

where EI is the flexural stiffness of the member. Eq.(18) then becomes

$$m = 1 - \frac{1}{(1+\psi/N)^2} \tag{25}$$

It is repeated that eq.(25) is not intended to produce results of a high degrees of accuracy as this can be better achieved by numerical integration. The purpose of eq.(25) is to provide a realistic closed solution.

Appendix A develops the actual section which corresponds to the m-ψ relation in eq.(25). It is seen to bear no resemblence to a wide-flange section. However, the important point is that it does represent a bi-symmetric section.

d) A CDC Equation

Two additional non-dimensional parameters will be introduced. A length parameter u where

$$u = \frac{x}{r_x} \cdot \sqrt{\frac{nN\epsilon_y}{2}} \tag{26}$$

where r_x is the in-plane radius of gyration and ϵ_y the yield strain, and a rotation parameter, a, where

$$a = \theta \cdot \frac{1}{f} \cdot \frac{M_p}{M_{pc}} \cdot \frac{d}{2r_x} \cdot \sqrt{\frac{n}{2N\epsilon_y}} \tag{27}$$

where f is the shape factor, M_p the plastic moment and d the depth of the member. With these substitions eq.(17) becomes

$$2u = \int_0^{\psi} \frac{dm}{\sqrt{a_0^2 - \frac{1}{N}\int_0^{\psi} \psi\, dm}} \tag{28}$$

Using the moment-curvature relation (eq. 25) gives

$$\sqrt{2}\, u = \int_0^{\psi} \frac{d\psi}{(1+\frac{\psi}{N})^3 \sqrt{\frac{a_0^2 N^2}{2} - \int_0^{\psi} \frac{\psi\, \psi}{(1+\psi/N)^3} d\psi}} \tag{29}$$

The interior integral is evaluated to give

$$u = \int_0^{1/1+\psi/N} \frac{\xi\, d\xi}{\sqrt{a_0^2 - (1-\xi)^2}} \tag{30}$$

where ξ is a dummy variable. The final integration gives

$$u = \sqrt{a_0^2 - \left(1 - \frac{1}{1+\frac{\psi}{N}}\right)^2} - a_0 + \arcsin \frac{1}{a_0} \frac{\psi/N}{1+\psi/N} \tag{31}$$

and from eq.(25)

$$u = \sqrt{a_0^2 - (1-\sqrt{1-m})^2} - a_0 + \arcsin \frac{1-\sqrt{1-m}}{a_0} \tag{32}$$

This is the CDC equation for the cross-section represented by eq.(25) (See Appendix A)

The equation is seen to be periodic with a half-wavelength, u_L, given by

$$u_L = \pi - 2a_0 \tag{33}$$

It is convenient to also have an equation for the CDC's with their origin at $u = u_L/2$. Calling these new co-ordinates $\bar{u}$ gives (from eq.(32))

$$\bar{u} = \frac{\pi}{2} - \sqrt{a_0^2 - (1-\sqrt{1-m})^2} - \arcsin \frac{1-\sqrt{1-m}}{a_0} \tag{34}$$

The two sets of CDC's represented by eqs.(32) and (34) are plotted in Fig. 5. It is seen that they closely resemble in form the CDC's derived numerically.[6,12]

The parameters m, a and u have been introduced as they produced significant simplifications in both the equations and their interpretation. Since these parameters may be unfamiliar, it is noted that m, a and u are proportional to M, θ and x and are defined in eqs.(21),(27) and (26) respectively.

The periodic portions of the CDC's can be found by taking non-principal values in eq. (32), for example

$$0 < u < u_L/2 \quad : \quad u = \sqrt{a_0^2 - (1-\sqrt{1-m})^2} - a_0 + \arcsin \frac{1-\sqrt{1-m}}{a_0} \qquad (35)$$

$$u_L/2 < u < u_L \quad : \quad u = -\sqrt{a_0^2 - (1-\sqrt{1-m})^2} - a_0 + \pi - \arcsin \frac{1-\sqrt{1-m}}{a_0} \qquad (36)$$

As eq.(25) is not valid for $\psi < 0$ (that is, it is not an odd function as is physically required), m should be replaced by $|m|$ in the above equations. However the periodicity of the CDC's means that if a quarter wavelength is known, this is sufficient to determine the entire function.

III THE COLUMN DEFLECTION CURVE EQUATIONS

a) Dependent Variables

An equation was derived in the preceding section (eq.(32)) for the CDC of a hypothetical section (Appendix A). This equation is plotted in Fig. 5 in terms of the three parameters m , a_o and u . In this form it is seen that the curves themselves are are independent of both the yield strain, ϵ_y , of the material and the axial force ratio, n , of the member. Thus the introduction of these three parameters produces a very significant simplification in the representation of the CDC's.

It is therefore of interest to see whether the same simplifications can be applied to the wide-flange CDC's. An examination of the derivation in Section II shows that this will be possible if the same m-ψ diagram will apply regardless of the values of ϵ_y and n . For yield strain, ϵ_y , this would be so if the residual strain patterns were proportional to the yield strain. This is not normally so[15] and therefore the simplification with respect to yield strain would need to assume that residual strain levels varied with yield strain. If the levels for A36 steel were used this assumption would be conservative and not very severe.

The situation with respect to axial load is more critical. The CDC solution would again be independent of axial load ratio (n) if the m -ψ relationships were similarly independent. This is not so; the higher the axial load ratio n the earlier the m -ψ curve will depart from the linear($m=\psi$) relation. The constant N was introduced into the assumed m -ψ relations (eq.25) to attempt to allow for this. The same constant then appears in the parameters a_o and u .

Thus it might be possible to similarly eliminate the axial load ratio from the real CDC's by introducing a term such as N which is related to the axial load ratio (compare with eq. 19)

b) Limit to CDC Equation

The slope of the CDC's is found by differentiating eq.(35), that is

$$\frac{dm}{da} = 2\sqrt{a_o^2 - (1-\sqrt{1-m})^2} = 2a \tag{37}$$

The maximum moment is therefore (at a=o)

$$1-\sqrt{1-m} = a_o \tag{38}$$

$$m_{max} = a_o(2-a_o) \tag{39}$$

Thus the maximum moment in the CDC increases parabolically with the end-deformation (a_o). But m cannot increase above unity, as at this value a limiting plastic hinge forms. Solving eq. (39) for m =1 gives a_o=1 as the deformation at which a hinge forms in the column.

It can be seen from Fig. 5 that at a_o=1 a plastic hinge does appear to form. This is contrary to some previous intuitive understandings[16] of the beam-column problem in which it was thought that the plastic hinge would be approached asymptotically. Actually the hinge will form at a finite deformation (a_o=1) and, following this, there will be an angular discontinuity at the hinge.

C) Post-Hinge Behavior

This behavior is diagramatically illustrated in Fig. 6. The angular discontinuity (or hinge angle, a_H)is found from eq.(37) with m=1 to be

$$a_H = 2\sqrt{a_o^2 - 1} \tag{40}$$

Similarly, the value of the half wavelength, u_L, is found from eq.(33) with m=1 to be

$$u_L = 2\left[\sqrt{a_o^2-1} - a_o + \arcsin\frac{1}{a_o}\right] \tag{41}$$

As a_o increases u_L will approach

$$u_L \rightarrow 2/a_o \tag{42}$$

In terms of the u co-ordinates (Fig. 5a) further deformations of the CDC after the hinge has formed will be due to rigid body rotations. That is, a mechanism approach may be used.[17]

The rotations of the member at a_o=1 are given by eq.(37) as $a_{(1)}$ where

$$a_{(1)}^2 = \sqrt{1-m}\left(2-\sqrt{1-m}\right) \tag{43}$$

For $a_o > 1$ the member rotations are then

$$a = a_o - 1 + a_{(1)} \tag{44}$$

Similarly the deformations at hinge formation are

$$u_{(1)} = a_{(1)} - 1 + \arcsin\left(1-\sqrt{1-m}\right) \tag{45}$$

and after hinge formation they are

$$u = u_{(1)} - \frac{m}{2}\left(1-\frac{1}{a}\right) \tag{46}$$

The hinge behavior explains why computer solutions to the wideflange CDC problem are not able to produce a complete quarter wavelength of a CDC for large values of a_o, regardless of the closeness of the steps used in the numerical integration. Clearly, the angular discontinuity (hinge) situation is reached. Figure 7 shows a plot of the value of a_o at which this computer inability was noted in programs run by the author. In evaluating a_o from the θ_o values and eq.(27), the value of N suggested by eq.(19) has been used. The section properties used correspond to 8WF31.

Considering the nature of the m-ψ hypothesis,(Fig. 4), the

agreement shown in Fig. 7 is good and indicates the validity of the preceding arguments.

d) Bending Assumptions

Two assumptions made in Section I were that (1) the curvature of the CDC could be expressed by the second derivative of the equation of the CDC and (2) that the curvature shortening of the member was small. Both these assumptions depend on the square of the slope of the deflection curve being small relative to unity.

The preceding section indicated that the maximum angle that could be expected in a CDC due to bending effects was given by $a_o=1$. This implies that, from eq. (27),

$$\theta \leq \sqrt{2\epsilon_y N} \cdot \frac{1}{\sqrt{n}} \cdot \frac{M_{pc}}{M_p} \cdot f \cdot \frac{d}{2h_x} \tag{47}$$

Assuming that M_{pc}/M_p is approximated by

$$\frac{M_{pc}}{M_p} = 1-n \tag{48}$$

and using eq.(19) and the 8WF31 section properties, reduces eq. (47) to

$$\theta \leq \sqrt{2\epsilon_y} \cdot \sqrt{\frac{2-n}{n}} \cdot (1-n) \cdot (1.28) \tag{49}$$

If $\theta^2 < 0.05$ be considered a suitable requirement then the restriction on the use of the CDC's is

$$2\epsilon_y \frac{2-n}{n} \cdot (1-n)^2 (1.28)^2 < \frac{1}{20}$$

or

$$\epsilon_y \frac{2-n}{n} (1-n)^2 < 0.015 \tag{50}$$

This relationship is plotted in Fig. 8. It is seen there that, for the commonly used steels, care should be taken in employing the CDC's at load ratio values below n=0.15

Note that although values of a_o larger than unity will occur once a hinge has formed these values will not be of consequence in any

bending action. In the post-hinge region the moments at the ends of the CDC's between the hinges will remain constant at m = 1 and further deformation increases will be a consequence of increases in the angular discontinuity at the hinge rather than of any further bending action.

A graph of the θ_o values corresponding to $a_o = 1$ is shown in Fig. 9. The graph is obtained from eq. (49). The assumption contained in eq. (9) that the slope of the CDC equals its gradient is within 5% accurate if the slope (θ) is less than 0.37 radian. It is seen from Fig. 9 that this assumption never becomes critical.

IV UNLOADING

a) History Dependence

In Section II(d) the concept of using different co-ordinate axes $(u,\bar{u})$ to represent the CDC's was introduced as a matter of mathematical convenience. In Fig. 5 it can be seen that the u axes correspond to one zero-moment point remaining fixed, whereas the $\bar{u}$ co-ordinates correspond to the column deforming symmetrically about a maximum moment point.

This choice of axes would remain a matter of algebraic convenience if the column material were not history dependent. However, the CDC properties are not invariant under the transformation of axes if the material is history dependent (as is structural steel).

The behavior can be illustrated by considering the history of the point of maximum moment on the $a_o = 0.25$ curves in both Fig. 5a(u) and Fig. 5b($\bar{u}$). In the $\bar{u}$ co-ordinates of Fig. 5b this point remains a point of maximum moment for all a_o and is continually loaded (the point remains at $\bar{u} = 0$). However for the u co-ordinates of Fig. 5a the maximum moment point for $a_o = 0.25$ is at $u = \pi/2 - 1/4 = 1.32$. As the deformation a_o is increased, m at u = 1.32 continues to rise to a maximum of around 0.7 and then drops. It is seen that at $a_o = 1$ the moment has even changed sign. This type of behavior requires a knowledge of the history dependence of the material.

For a material such as structural steel the initial unloading will be elastic. (Fig. 10) The arrows in Fig. 10 represent the direction of loading. For a virgin material, eq. (25) holds if d is positive, i.e.

$$dm > 0, \qquad m = 1 - \frac{1}{(1+\psi/N)^2} \tag{25}$$

and for any unloading and reloading

$$\frac{dm}{d\psi} = \frac{2}{N} \tag{51}$$

The use of eqs. (25) & (51) will result in different CDC's being obtained for different axes. This point is illustrated in Fig. 11 which shows the variation in unloaded regions for two indentical CDC's drawn to the u and $\bar{u}$ axes. The regions shown in Fig. 11 will later be seen to be non-inclusive.

For a given location on the CDC, unloading will occur once the moment at this point begins to decrease as a_o increases. But this also defines the envelope of the CDC's. That is, for all choices of axes, unloading at a point will occur once the CDC at that point reaches the CDC envelope for the particular set of axes under consideration.

Obviously, the above discussion of unloading applies to the CDC's derived for both the real and the hypothetical sections. The following discussion of envelopes will be particularized to the hypothetical section.

b) Algebraic Formulation

The envelopes for the CDC's are found by obtaining $\frac{\partial m}{\partial a_o}$ for a constant u or $\bar{u}$. For the hypothetical curves, eq. (36) gives (for the u axes)

$$u: \quad \frac{\partial m}{\partial a_o} = 2\left[\frac{a_o^2 - (1-\sqrt{1-m})}{a_o} - \sqrt{a_o^2 - (1-\sqrt{1-m})^2}\right] \tag{52}$$

similarly, for the $\bar{u}$ axes

$$\bar{u}: \quad \frac{\partial m}{\partial a_o} = 2\left[\frac{a_o^2 - (1-\sqrt{1-m})}{a_o}\right] \tag{53}$$

The envelope is at $\frac{\partial m}{\partial a_o} = 0$, that is at

u: $$a_o^2 = \frac{1-\sqrt{1-m}}{1+\sqrt{1-m}} \tag{54}$$

ū: $$a_o^2 = 1-\sqrt{1-m} \tag{55}$$

These parametric equations are converted into envelope equations by substituting into eqs. (34) and (36),

u: $$\begin{cases} \frac{\pi}{2} > u > \left(\frac{\pi}{2}-1\right) & u = \pi - \sqrt{m_e} - \arcsin\sqrt{m_e} \quad (56) \\ \left(\frac{\pi}{2}-1\right) > u > 0 & m_e = 1 \quad (57) \end{cases}$$

ū: $$\pi/2 > \bar{u} > 0. \qquad \bar{u} = \frac{\pi}{2} - \sqrt{1-m_e} - (1-m_e) - \arcsin\sqrt{1-\sqrt{1-m_e}} \tag{58}$$

The two sets of envelopes are shown by dashed lines in Figs. 5a and 5b. They are also plotted separately in Fig. 12.

As well as giving the point at which unloading commences, the envelope also gives the moment at that point. For example, the value of m_e shown in Fig. 10 is the value of m_e on the envelope at the corresponding (generalized) u location. The value of ψ_e is obtained from eq. (25). Thus eq. (51) may be integrated to give the unloading m-ψ curve:

$$m - m_e = \frac{2}{N}(\psi - \psi_e) \tag{59}$$

This equation implies that the amount of unloading ($|m-m_e|$) is sufficiently small to prevent any yielding in the reverse direction.

In finding the equations for the CDC's subjected to unloading it is simpler to use the differential, rather than the intergral, form of the equilibrium equation (eq. (8) rather than (28)) as m_e and ψ_e are both functions of u. Eq. (8) becomes

$$m - \frac{2}{N}\psi = m_e - \frac{2}{N}\psi_e \tag{60}$$

Using eq. (26) and writing $\frac{d^2m}{du^2} = m''$ gives

$$m'' + m = m_e - \frac{2}{N}\psi_e \tag{61}$$

Now eq. (61) leads to an interesting interpretation, for if the symbol Δm is introduced where

$$\Delta m = \frac{2}{N}\psi - m \tag{62}$$

eq. (61) becomes

$$m'' + m = \Delta m \tag{63}$$

But Δm is a simple property of the moment-curvature curve and is shown in Fig. 13 to be the distance between the ideal elastic and the real m-ψ curve. As m_e is known as a function of u (eqs. 56-58), Δm is also known as a function of u.

The solution of eq. (63) is[18]

$$m = C \sin u + B \cos u - \int \Delta m(\xi) \sin(u - \xi)\, d\xi \tag{64}$$

where C & B are constants and ξ is a dummy variable. It is emphasized that eq. (64) applies to any CDC, the section properties loading history and m-ψ relation only enter via the term Δm inside the integral on the RHS of the expression and the constants C & B.

c) Numerical Solution

The numerical integration solution to the problem is relatively simple. The integration is commenced at a point known to have undergone no unloading (for example, the maximum moment point with the u axes). Integration then proceeds until the envelope is reached. (Point T in Fig. 14) If it is assumed that a point P (Fig. 14) is reached it is necessary to find the curvature at P. The moment at P is Fy_p and from the envelope the envelope moment is Fy_{ep}. The drop in moment is then $F(y_{ep} - y_p)$ and the elastic curvature drop is

$F(y_{ep}-y_p)/EI$. Hence the actual curvature at P is

$$\phi = \phi_{ep} - F(y_{ep}-y_p)/EI \tag{65}$$

where ϕ_{ep} is the loading curvature corresponding to the moment Fy_{ep} . Hence the standard numerical integration procedure[6] can be followed with the normal moment-curvature data replaced by equation (65).

Such CDC curves have been computed by the author for the $\bar{u}$ case (Fig. 5b). In this situation there is little difference between the loading and unloading curves. There are two related reasons for this. Firstly, the regions that do unload are the less highly loaded portions of the CDC (see Fig. 11a) and, secondly, most of the deformation of the column continues to come from regions under monotonic loading.

Figure 15 illustrates the actual result obtained from one numerical calculation. It will be realized from Fig. 10 that, for the same moment drop, the curvatures in the "unloading" CDC will be greater; hence it will deform more rapidly. The effect of this behavior on beam-column response will be discussed later.

d) Algebraic Solution

The algebraic solution of eq. (64) is complicated by the difficulty in evaluating the integral term in the equation. From eq. (62) and (25), Δm is given by

$$\Delta m = \frac{2}{\sqrt{1-m_e}} - 2 - m_e \tag{66}$$

The value of m_e is found from eq. (58). The combination of eqs. (58) and (66) in eq.(64) leads to a quite intractable integral. There is little point in resorting to a numerical solution to this integral when the actual problem can be more simply solved by the numerical procedures in the

preceding sub-section. Therefore the algebraic solution of the unloading of the hypothetical CDC's will not be pursued any further.

However the form of the solution given in eq. (64) does illustrate an important point. The first two terms on the right hand side of the equation correspond to the elastic solution. The integral term is the modification due to the residual curvatures remaining from prior loadings. Thus the unloading curve is <u>not</u> an elastic curve, although it contains an elastic component.

V THE DESIGN PROBLEM

a) Review

Section I discussed how a beam-column (Fig. 1a) could be represented as part of a column deflection curve (Fig. 2b). This allows considerable simplifications to beam-column design.

For a beam-column under the loads P, M_L, M_R & V shown in Fig. 1a the corresponding CDC is one loaded by a force F where

$$F = P \cdot \sqrt{1 + \left(\frac{M_R - M_L}{P\ell}\right)^2} \tag{67}$$

The CDC representation should be used with care for values of F below the levels given in Fig. 8. The length ℓ of the beam-column is adjusted to a length ℓ' along the F-axis of the CDC (Fig. 2b), where

$$\ell' = \ell \sqrt{1 - \left(\frac{M_R - M_L}{P\ell}\right)^2} \tag{68}$$

In most cases the quantity

$$\left(\frac{M_R - M_L}{P\ell}\right)^2$$

appearing in eqs. (67) and (68) will be quite small relative to unity. Thus the correction in eqs. (67) and (68) can be assumed to be

$$\pm \frac{1}{2}\left(\frac{M_R - M_L}{P\ell}\right)^2$$

If a 5% error is tolerable, eqs. (67) and (68) need only be used when

$$\frac{M_R - M_L}{P\ell} \geq \frac{1}{\sqrt{10}} = 0.32 \tag{69}$$

The situation is obviously most severe for short beam-columns in double curvature, under low axial loads.

The process of locating beam-column segments on a CDC has been fully dealt with elsewhere[4,6,12,19] and will not be discussed here. However it is noted that the $\bar{u}$ axes (Fig. 5b) are convenient for representing beam-columns under equal end moments and the u axes (Fig. 5a)

for representing beam-columns with one end pinned or with equal and opposite end-moments. These representations are illustrated in Fig. 16.

All the above remarks apply equally to both the real and hypothetical CDC's.

b) Interaction Diagrams

Interaction curves for beam-columns relate the maximum end-moment that the member can carry to its other physical parameters. For the three loading cases shown in Fig. 16 the maximum moment is also the envelope moment for the relevant set of axes. That is, the envelopes given previously in Figs. 5 and 12 are also the interaction diagrams for the relevant loading cases.

In Fig. 12 the entire set of interaction diagrams for the hypothetical section are represented by a single curve for each loading condition. This represents a considerable simplification on present interaction diagrams. Both axial load and yield stress are introduced through the parameters m and u. (eq. (21) & (26)).

As was the case for the single CDC representation (Section IIIa), the above conclusion will also apply to real beam-columns if the relations do not depend on yield stress or axial load. This will be approximately so for yield stress, but will not be the case for variations in the axial load ratio. In this latter instance it may be possible to introduce a factor similar to N appearing in the u parameter (eq. (26)).

c) Moment-Rotation Curves

The end-moment vs end-rotation curves for a beam-column may also

be derived from the CDC's[6,12,19]. As an example, the curve for equal end moments ($\bar{u}$ axes) for the hypothetical section will be derived. In this case (Fig. 16c) the slope of the CDC is also the end-rotation of the beam-column. From eq. (37) this slope is

$$a^2 = a_o^2 - (1-\sqrt{1-m})^2 \tag{70}$$

Thus the paremeter a_o can be removed from eq. (34) to give

$$\bar{u} = \frac{\pi}{2} - a - \arctan\frac{1-\sqrt{1-m}}{a} \tag{71}$$

or

$$m = a\cot(a+\bar{u})\cdot(2-a\cot(a+\bar{u})) \tag{72}$$

Writing

$$\alpha = a\cot(a+\bar{u}) \tag{73}$$

gives

$$m = \alpha(2-\alpha) \tag{74}$$

which is plotted in Fig. 17a and represents the moment-rotation curve.

Figure 17a is independent of yield stress, axial load ratio and slenderness ratio and applies only to the hypothetical CDC's. When applied to real sections the simplification with respect to yield stress and axial load ratio will again depend on the constancy of the diagram $(m-\psi)$. However, the slenderness ratio simplification - introduced through the parameter α - is valid for all sections and derivations.

Figure 17b shows the same moment-rotation curve, but this time plotted as m vs. a rather than m vs. α. It is seen that the curves must now each be plotted for a separate slenderness ratio parameter ($\bar{u}$). The curve for $\bar{u} = 0$ provides an envelope to the other curves. The point of hinge formation is also noted ($a_o = 1$) on Fig. 17b. It is interesting to note the similarity of this curve to previously predicted[20] curves for the point of local buckling.

d) Post-Hinge Moment-Rotation Curves

The behavior after the point of hinge formation ($a_o = 1$) can

be predicted using the post-hinge study of Section IIIc. The present situation is illustrated in Fig. 18. The column under consideration is of length $2\bar{u}$. At the point of hinge formation it has an end-moment $m_{(1)}$ and an end-rotation $a_{(1)}$. A rigid body rotation occurs about the hinge. Using eq. (37) to relate m, u & a the moment m is related to the rotation a by

$$a - a_{(1)} = -\frac{1}{2}\frac{m - m_{(1)}}{\bar{u}} \tag{75}$$

or

$$m = m_{(1)} - 2\bar{u}\,(a - a_{(1)}) \tag{76}$$

An example of the use of eq. (76) is given in Fig. 19. The beam-column chosen has a length of $2\bar{u} = 0.8$ (see Fig. 17b). For a $P/P_y = n = 0.5$ and $\epsilon_y = .0012$ this corresponds to a slenderness ratio of 32. From eqs. (70) & (72) it is found that the values of $m_{(1)}$ and $a_{(1)}$ for this case ($\bar{u} = 0.4, a_o = 1$) are 0.352 and 0.973 respectively. Eq. (76) is now

$$m = 1.30 - 0.8a \tag{77}$$

which is plotted in Fig. 19. This behavior has been substantiated by recent test results.[21]

It is relevant to note that the mechanism curve is stiffer than the pre-hinge curve. This is a result of the absence of further flexural deformations.

Further deformation will continue along the mechanism curve until M_{pc} is reached at the ends of the member. This behavior is illustrated in Fig. 20. It can be seen that the negative end-moment reaches a greater value (m = 1) then the initial positive end-moment. Eventually the CDC acts in a concertina fashion and the moment-rotation

curve spirals around the m-a origin in a clockwise direction. Similar curves to this have been produced analytically[7], however, it was not recorded how the computer was able to handle the angular discontinuities at the hinges. Thus the actual analysis is open to some question[22].

e) Unloading of the Moment - Rotation Curves

The problem of unloading was discussed in Section IV. The effect on the CDC's was shown in Fig. 15. This effect of unloading on beam-column behavior may be illustrated by considering the example of the beam-column under equal end-moments ($m_L = m_R$) discussed previously. The situation is shown in Fig. 21a.

The points plotted on a moment-rotation (m-a) curve are the points corresponding to the points N (no-unloading) and U (unloading) in Fig. 21a. The m-a curve is shown in Fig. 21b. From Section IV it is known that unloading begins after the CDC has reached its envelope, but from Section Vb it is also known that the end-moment also begins to drop at this same point. Therefore it may be concluded that the point of unloading of the entire beam-column begins at the same point as the end-moments begin to unload ($m_L = m_R$) (Fig. 21b).

Within the idealized assumptions used to derive the post-hinge curve, unloading plays no part. Therefore, the range to be considered is between the peak of the moment-rotation curve and the point of hinge formation.

Now if the point N is plotted on the m-a curve (Fig. 21b), it can be seen from Fig. 21a that the point U must be for a lower moment and a larger rotation. Consequently U will move from N in a direction similar to the direction of the m-a curve. This indicates that unloading will have only minor effects on the behavior of beam-columns with equal end-moments. Fig. 22 illustrates this for an actual case.

No attempt has been made in this section to generalize the results to all loading cases. Rather, an attempt has been made to illustrate those problems which are of consequence for one loading case. The methods by which this case has been solved are then applicable to the other loading cases.

f) Lateral Loads

The CDC concept can also be used to predict the behavior of beam-columns with intermediate lateral loads. The approach used in these cases is illustrated in Appendix B.

VI STABILITY

a) Introduction

It is meaningless to speak of the stability or otherwise of an individual member, unless the response of its load system to deformation is also specified.[23] The point of instability occurs when the combined structure and load system offer no resistance to imposed disturbances. The common statement[5,13] that a beam-column becomes unstable when it reaches the peak of its moment-rotation curve is seen to be true only when the member is directly loaded by gravity loads.

It will be realized, however, that a knowledge of the load-deformation response of both the beam-column and the load system is sufficient to allow the determination of the point of in-plane instability of a system. The method[23] is illustrated in Fig. 23.

A study of curves such as Figs. 17b, 19 & 22 leads to the conclusion that in many practical cases the unloading portion of the moment-rotation curves is too flat to allow any in-plane instability to occur. This surmise is supported by a number of beam-column tests[21,24], all of which exhibited an entirely stable load history.

b) Inherent Instability

Instability within a member is precluded as the CDC's are based on the solution of an equilbrium equation ((8)). Therefore, any local accelerations will be transmitted to the joints, and the problem will be again one of overall instability.

It might be noted here that the entire report ignores the possibilities of either local or lateral buckling[20,23].

c) Deformation Mode Instability (Double Curvature)

If the behavior of a beam-column is followed from its zero load position by choosing segments from the CDC's, an equilibrium moment-rotation curve will be obtained which can be checked for instability by the methods of sub-section (a) above. In any real situation the moments applied will be such as to produce components of the two prime deformation modes (single and double curvature). The points on the moment-rotation curve will therefore be unique for a monotonic loading from zero deformation.

However, in exceptional cases this will not be true. If the beam-column is loaded in perfect double curvature ($m_L + m_R = 0$) the single curvature mode of deformation will not be present. In this case the load-deformation path will not be unique as a stage will be reached at which the member will also be able to adopt a predominantly single curvature deformation mode. When this change of modes is possible and occurs, the phenomenon is known as "unwinding". It has recently been discussed by Ketter[25,27] and Ojalvo[26].

The problem is essentially a buckling problem as has been pointed out by Bijlaard[9b]. The double curvature column buckles or bifurcates towards a single curvature mode (Fig. 24a) with the change in shape rather than the final shape being important. For a simple case Bijlaard[9b] showed that this change was in itself a single curvature mode. The bending moment diagram is shown in Fig. 24b. Bifurcation will be expected under tangent modulus conditions[28] and so the stiffness distribution will be as shown in Fig. 24(c)[26,27]. Ketter[25] illustrated a method of solving this problem and gave[27] the solution to one case.

Ojalvo[26] has attempted a proof that a beam-column will only be stable if its length is less than the half wavelength of the CDC. This proof is not valid for the exceptional case of the beam-column under equal and opposite end moments, and seems irrelevant for other cases. Figs. 24(d) & (e) relate the points on the moment-rotation curve to CDC segments. The only way to check the possibility of such segments bifurcating is to use Ketter's method[25,27]. Ojalvo's proof (Fig. 20c, Ref. 21) is seen to break down if the end-moments are equal.

A comparison of Figs. 24(d) and (e) illustrates that unwinding may conceivably not occur until after the end-moments have begun to decrease.

In conclusion, it should be stated that the problem of unwinding is an academic one; its relation to real structures is similar to the relation of simple buckling to real columns. The analytical problem described above can be circumvented by the simple process of assuming that the end-moments are not quite equal (the difference is determined by the accuracy of the available CDC data). This forces the beam-column to have a single curvature component from the outset of loading. Thus the correct solution is obtained directly from the moment-rotation curve without any need to undertake buckling analyses.

e) Deformation Mode Instability (General Problem)

A more real problem than that considered above concerns the selection of a CDC segment to satisfy a given set of moments, forces and length. As the CDC wavelength decreases with deformation (Fig. 5), it is seen that there is an infinite set of segments which will satisfy a given loading (see Fig. 20, for example).

Under normal conditions only one or two of these configurations

will ever be attained during a stable loading process and the problem is to determine whether a chosen configuration falls into this category. Complex criteria could be advanced to meet this requirement, however a much simpler method exists.

The method advocated is to begin all beam-column analyses from the unloaded condition, tracing the entire moment-rotation curve up to the point required. This will ensure that a realistic mimumum energy configuration is obtained if the following provisoes are followed:

1) The initial length of the beam-column must be less than its Euler buckling length,
2) The moments must contain some component of the single curvature loading condition

Provisoe (1) restricts the first segment chosen to the lowest energy configuration of all the initial members of the possible set and provisoe (2) ensures that the segments chosen during the tracing of the loading path remain realistic.

This section has avoided calling segments stable or unstable as a segment which is unstable under one type of loading can be stable under a loading with a different load-deformation response. Stability is a function of both the member and its load system[23].

VII CONCLUSIONS

This report has examined the properties of the column deflection curves, both as individual functions and as a source of beam-column information. This examination has been aided by the development of an algebraic expression for the column deflection curves of a hypothetical section.

The necessary requirements for representing a beam-column as part of a column deflection curve have been delineated.

With the aid of the algebraic solution various new CDC parameters have been found. The use of these non-dimensional parameters make it possible to very considerably reduce the amount of data needed to represent the column deflection curves, the beam-column moment-rotation curves and the beam-column interaction diagrams.

The formation of hinges in beam-columns has been discussed and analytically described. It was shown that a simple assumption suffices to represent the behavior of a beam-column once a hinge has formed within its length.

The problem of unloading of yielded sections has been discussed. Computations have been presented to indicate the magnitude of its effect. It was shown that there is a close relation between the interaction diagrams, the CDC evelopes, and the points of unloading.

Finally the stability of beam-columns has been investigated. It was concluded that the stability or otherwise could be investigated by relatively simple methods.

The general study of column deflection curve behavior appears to have led to a simplification and advancement of present knowledge on this topic.

VIII ACKNOWLEDGEMENTS

The writer wishes to acknowledge the kind help and assistance that he has received from Professor T. V. Galambos throughout the proparation of this report. This work has been carried out as part of an investigation sponsored jointly by the Welding Research Council and the Department of the Navy with funds furnished by American Institute of Steel Construction, American Iron and Steel Institute, Institute of Research, Lehigh University, Column Research Council (Advisory), Office of Naval Research (Contract No. 610 (13)), Bureau of Ships, and Bureau of Yards and Docks.

Professor W. J. Eney is Head of the Civil Engineering Department, and Professor L. S. Beedle is Director of the Laboratory.

The report was typed by Miss N. Turner and Mr. R. J. Weiss and Mr. H. A. Izquirdo did the drawings.

IX APPENDIX A

SECTION GIVING THE HYPOTHETICAL MOMENT-CURVATURE RELATION

Consider the general section shown in Fig. A1. The internal moment is given by

$$\frac{M_i}{4} = \int_0^{\epsilon_y/\phi} E\phi y \cdot x \cdot y\,dy + \int_{\epsilon_y/\phi}^{\infty} \sigma_x \cdot x \cdot y\,dy \tag{A1}$$

$$= E\phi\, I_1\Big|_0^{\epsilon_y/\phi} + \sigma_y\, I_2\Big|_{\epsilon_y/\phi}^{\infty} \tag{A2}$$

where

$$I_1 = \int y^2 x\,dy = I_1(y) \tag{A3}$$

and

$$I_2 = \int y x\,dy = I_2(y) \tag{A4}$$

$$\therefore \quad \frac{M_i}{4} = E\phi\left[I_1\left(\frac{\epsilon_y}{\phi}\right) - I_1(0)\right] + \sigma_y\left[I_2(\infty) - I_2\left(\frac{\epsilon_y}{\phi}\right)\right] \tag{A5}$$

Now, taking $\frac{\partial}{\partial\phi}$ of eq.(A5) and utilizing eqs.(A3) and (A4) gives

$$\frac{1}{4}\frac{\partial M_i}{\partial\phi} = E\left[I_1\left(\frac{\epsilon_y}{\phi}\right) - I_1(0)\right] \tag{A6}$$

But from eq.(18)

$$\frac{\partial M_i}{\partial\phi} = \frac{2EI}{N} \cdot \frac{1}{(1+\Psi/N)^3} \tag{A7}$$

Equating (A5) & (A6) gives

$$\frac{2I}{N} \cdot \frac{1}{\left(1+\frac{\phi}{N\phi_{pc}}\right)^3} = I_1\left(\frac{\epsilon_y}{\phi}\right) - I_1(0) \tag{A8}$$

Taking $\frac{\partial}{\partial\phi}$ of this equation,

$$\frac{6I}{N^2} \cdot \frac{EI}{M_{pc}} \cdot \frac{1}{\left(1+\frac{\phi}{N\phi_{pc}}\right)^4} = \frac{1}{\epsilon_y}\left(\frac{\epsilon_y}{\phi}\right)^4 x\left(\frac{\epsilon_y}{\phi}\right) \tag{A9}$$

Replacing ϵ_y/ϕ by the variable y gives

$$x = x(y) = \frac{6I}{N} \cdot \left(\frac{I\sigma_y}{NM_{pc}}\right) \cdot \frac{1}{\left(y+\frac{I\sigma_y}{NM_{pc}}\right)^4} \tag{A10}$$

which is the cross-sectional shape corresponding to the assumed relation, eq.(18). Putting

$$\beta = \frac{I\sigma_y}{NM_{pc}} \tag{A11}$$

and

$$\gamma = \frac{6N^2M_{pc}^3}{I^2\sigma_y^3} \tag{A12}$$

reduces eq. (A10) to

$$x = \frac{\gamma}{\left(1+\frac{y}{\beta}\right)^4} \tag{A13}$$

which is plotted in Fig. A2.

APPENDIX B

BEAM-COLUMNS WITH LATERAL LOADS

Contrary to some previously expressed opinions, there is no significant difficulty associated with treating the laterally loaded beam-column (Fig. B1a) by the CDC approach. The solution will be illustrated for the one lateral load case shown in Fig. B1a. The deflection at the lateral load is called δ_c . The solution is obtained by treating the member as two beam-columns, LC & CR. As an example, the member LC is shown in Fig. B1b.

Under normal conditions the axial load can be taken as remaining equal to P. The moment at C is M_C and is given by

$$M_c = M_{CK} + P\delta_c \tag{B1}$$

where M_{CK} is independent of δ_c and is given by

$$M_{CK} = QL\alpha(1-\alpha) + M_R\alpha + M_L(1-\alpha) \tag{B2}$$

It is not usually necessary to determine R_1.

The solution may proceed as follows. The values of P, M_L, M_R, L & α are known. It is desired to find the conditions (if any) corresponding to a chosen load Q. A value of δ_c is assumed (this choice will be discussed later) and hence, M_C is determined. The CDC's are then used to find a beam-column under the loading shown in Fig. B1b for LC and a similar column for RC. The angles θ_{cL} and θ_{cR} are thus determined.

If the choice of δ_c was correct, then continuity at C will require the following equation to be true

$$\theta_{cL} + \theta_{cR} = \frac{\delta_c}{L\alpha(1-\alpha)} \tag{B3}$$

If it is not, a new value of δ_c is chosen and, by trial and error, eq.(B3) is satisfied. However, in those cases where the value chosen for Q is above the maximum value that can be carried, no solution is possible and it is necessary to choose a smaller value in order to satisfy eq.(B3).

The selection of Q and δ_c values can be simplified by first constructing the elastic and the mechanism curves. Such a plot is shown in Fig. B2. The elastic curve is obtained from standard texts, δ_{co} being the beam-column deflection of C when Q is zero. The value of Q_ϕ (Fig. B2) is the rigid-plastic value and, if M_L and M_R are below M_{PC}, is given by eq. (B1) with $\delta_c = 0$. This reduces to $M_{CK} = M_{PC}$. Similarly, $\delta_{c\phi}$ in Fig. B2 is for $Q = 0$ at mechanism formation and is again found from eqs. (B1) and (B2), this time with $Q=0$ and $M_C = M_{PC}$. The two curves in Fig. B2 greatly facilitate the selection of realistic Q and δ_c values.

As an example of the process, Fig. B3 gives the solution of a specific problem. A value of Q (say, 5 kip) is chosen and eq. B2 evaluated to give M_{CK} (602 kip-in). A value of δ_c is then selected (say, 0.6 in) and eq.(B1) used to find M_C (681 kip-in or 0.690 M_y). The CDC's are searched to find a beam-column of length $20r_x$, $P = 0.4P_y$ and end-moments M_C and M_L (0.690 M_y & 0.434 M_y). This member is found to have a rotation at C of θ_c (0.0075) and so ($\theta_c + \theta_R$) is known (0.0150). But the right hand side of eq. B3 is found from δ_c (0.0172). These are generally not equal and so a new δ_c value is selected ($\delta_c = 0.5''$).

X NOMENCLATURE

A	cross-sectional area
B	constant
C	constant
CDC	column deflection curve
E	modulus of elasticity
EI	flexural stiffness
F	CDC force
F_y	A σ_y
I	second moment of area
L	left end of beam-column
M	moment
M_C	moment at a lateral load point
M_{CK}	component moment, eq. B2
M_i	internal moment
M_L	moment at left end of beam-column
M_P	plastic moment
M_{pc}	plastic moment reduced by axial load
M_R	moment at right end of beam-column
N	constant in moment-curvature equation
P	beam-column axial load
Q	lateral load
V	shear
a	rotation parameter, eq. 27.
a_o	deformation parameter (angle between CDC and F axis)

$a_{(1)}$	CDC rotation parameter at point of hinge formation
a_H	hinge angle parameter
d	depth of section
f	shape factor
ℓ	undeformed length of a beam-column
ℓ^*	chord length of a deformed beam-column
ℓ'	beam-column length along CDC F-axis
m	moment ratio, M/M_{pc}
m_e	moment ratio on CDC envelope
m_L	moment ratio at left end of beam-column
m_R	moment ratio at right end of beam-column
m^{11}	d^2m/du^2
Δm	property of m-γ curve, eq. 62
n	force ratio, F/F_y
r_x	in-plane radius of gyration
u	length parameter, eq. 26
$\bar{u}$	length measured from maximum moment location
u_L	CDC half-wavelength in terms of u
$u_{(1)}$	CDC deformations when a hinge forms
v	beam-column deflection
w	distance along a beam-column
x	distance along F-axis
y	deflection of CDC from F-axis
y_p	CDC deflection at a point P
y_{ep}	location of CDC envelope at a point P

α	location of a lateral load moment-rotation parameter, eq. 73
β	section property, eq. A11
γ	section property, eq. A12
ϵ_y	yield strain
θ	CDC slope
θ_c	rotations at a lateral load
θ_o	CDC slope at F-axis
ω	angle between F-axis and beam-column (LR)
η	E axis location parameter, eq. 3
ϕ	curvature
ϕ_{ep}	envelope curvature at a point P
ϕ_{pc}	elastic curvature corresponding to M_{pc}
ψ	curvature ratio, ϕ/ϕ_{pc}
ψ_e	curvature ratio on CDC envelope
σ_y	yield stress
ξ	dummy variable
δ_c	deflection at a lateral load point

XI FIGURES

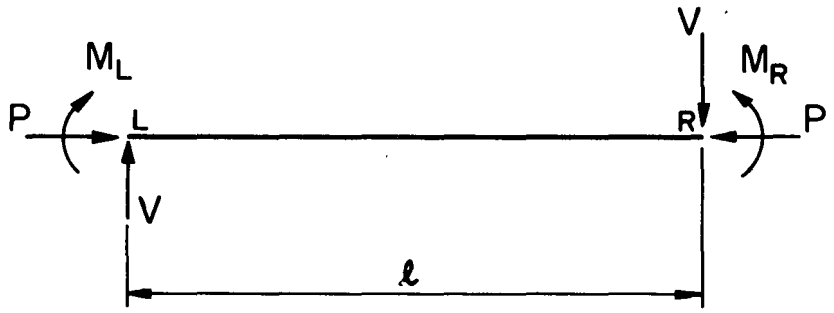

Fig. 1a Loads On An Undeformed Member

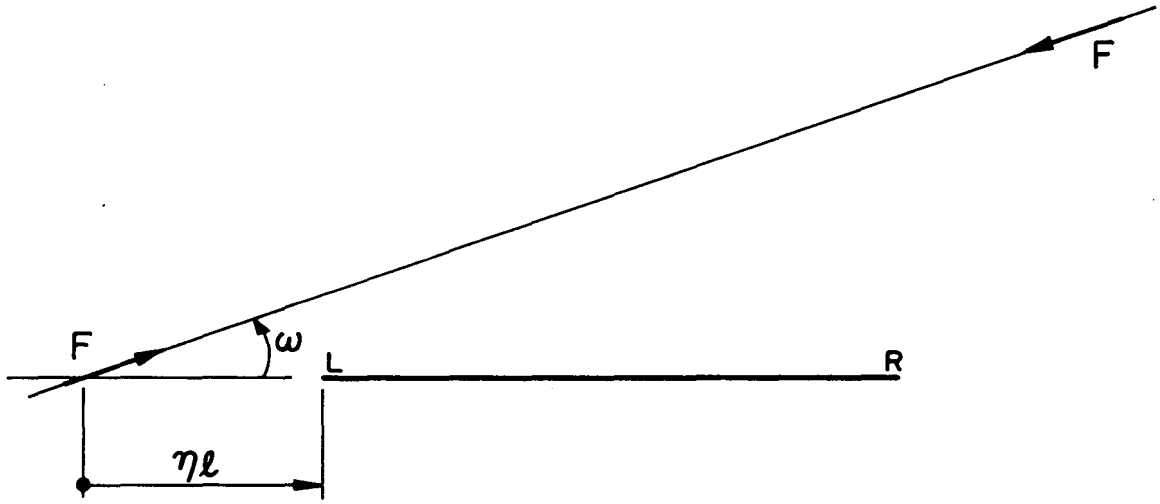

Fig. 1b System Equivalent To Fig. 1a

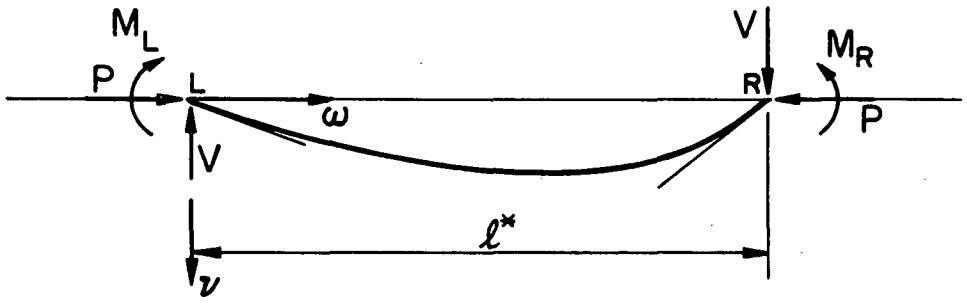

Fig. 2a Deformed Loaded Member

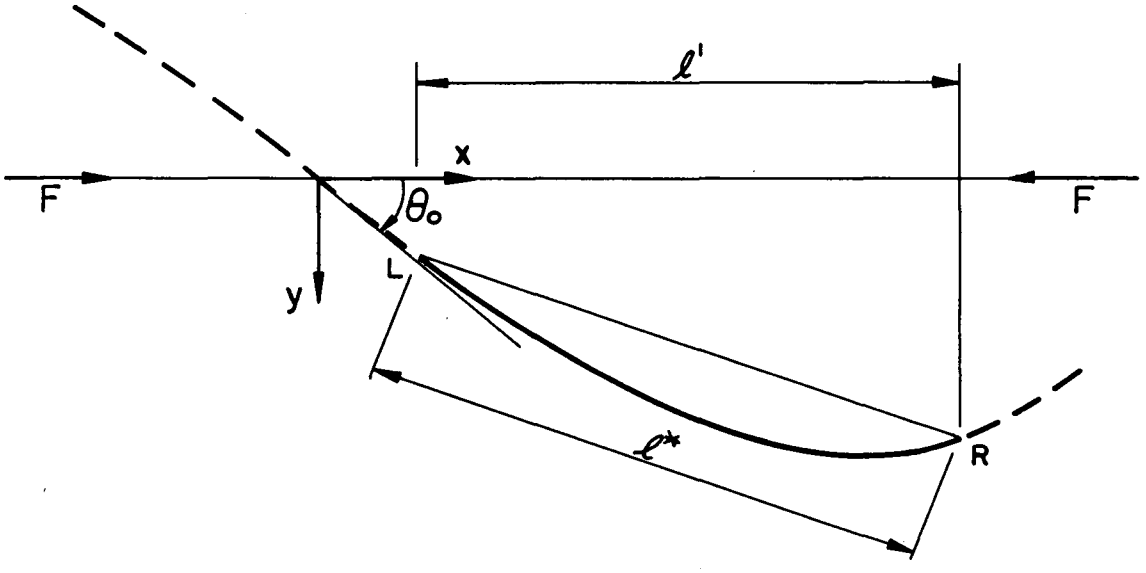

Fig. 2b Deformed System Equivalent To Fig. 2a

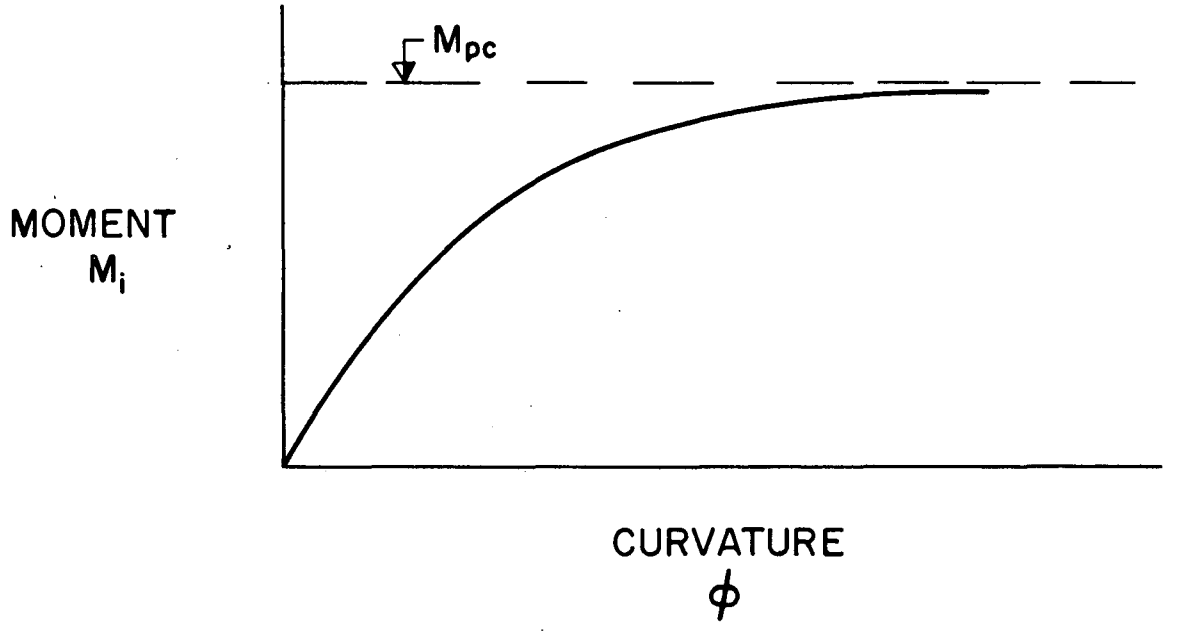

Fig. 3 Required Form Of Moment-Curvature Relation

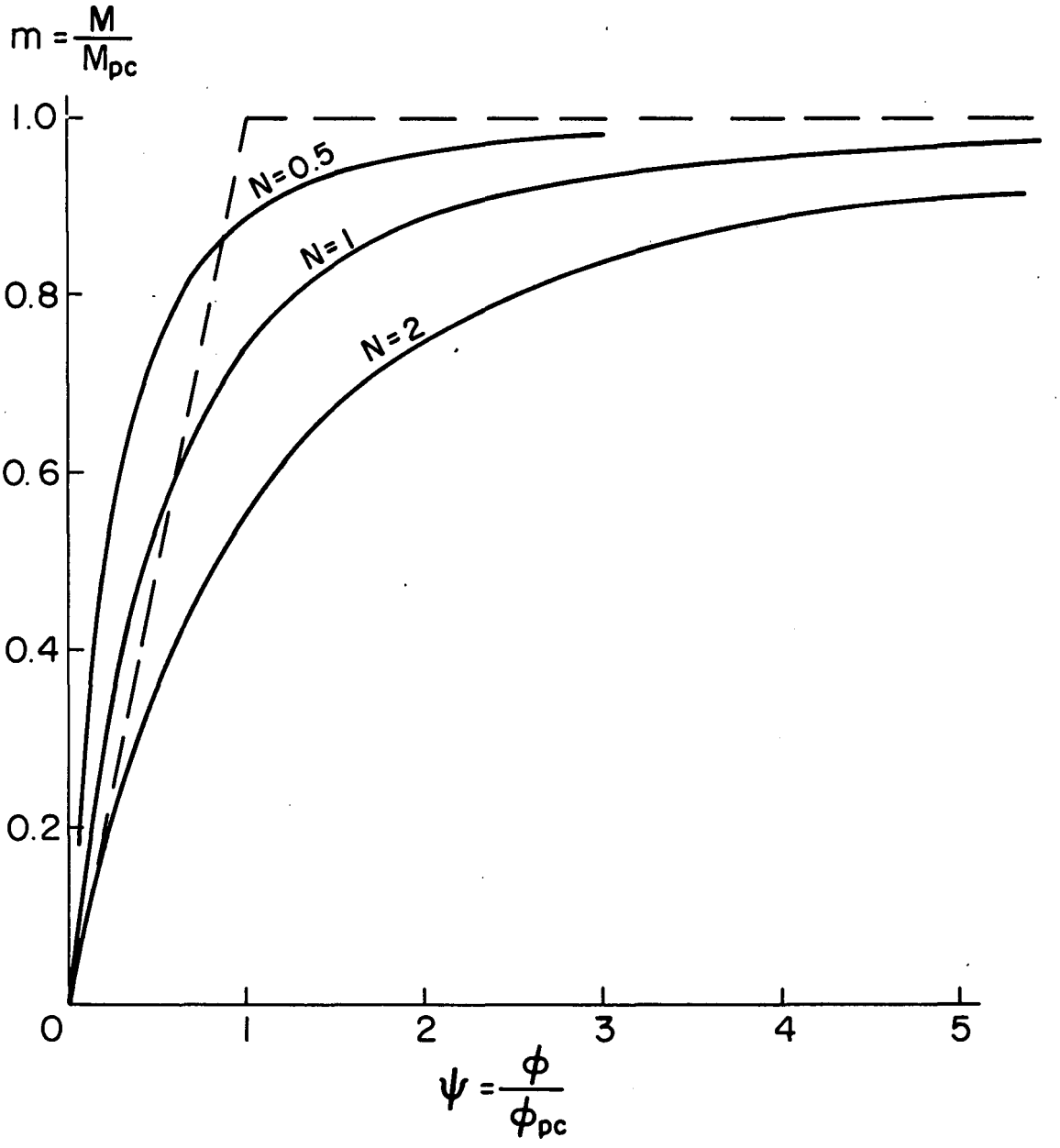

Fig. 4 Assumed Moment-Curvature Relation

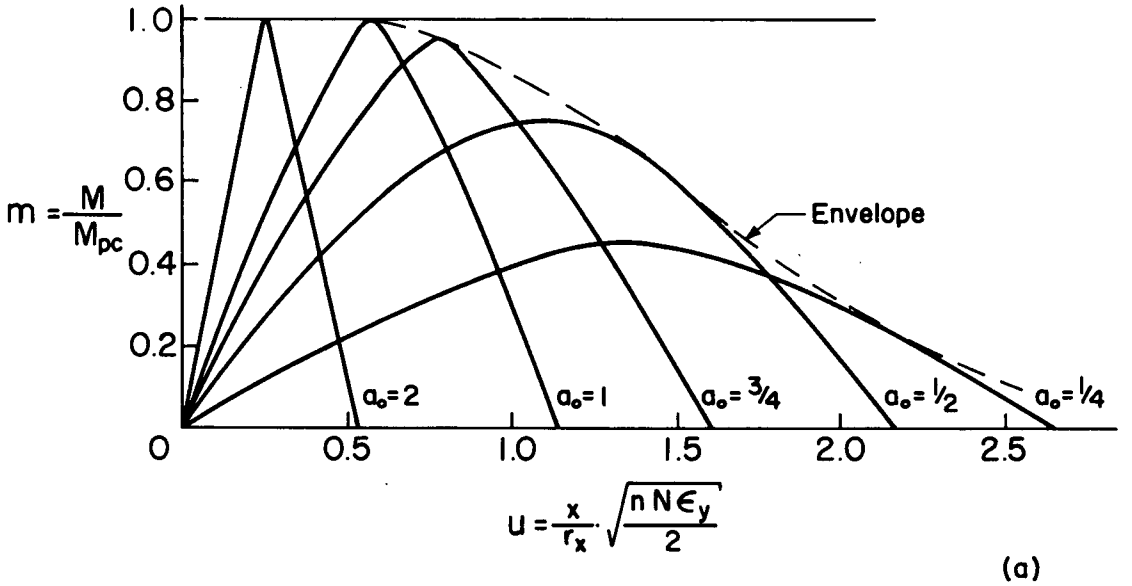

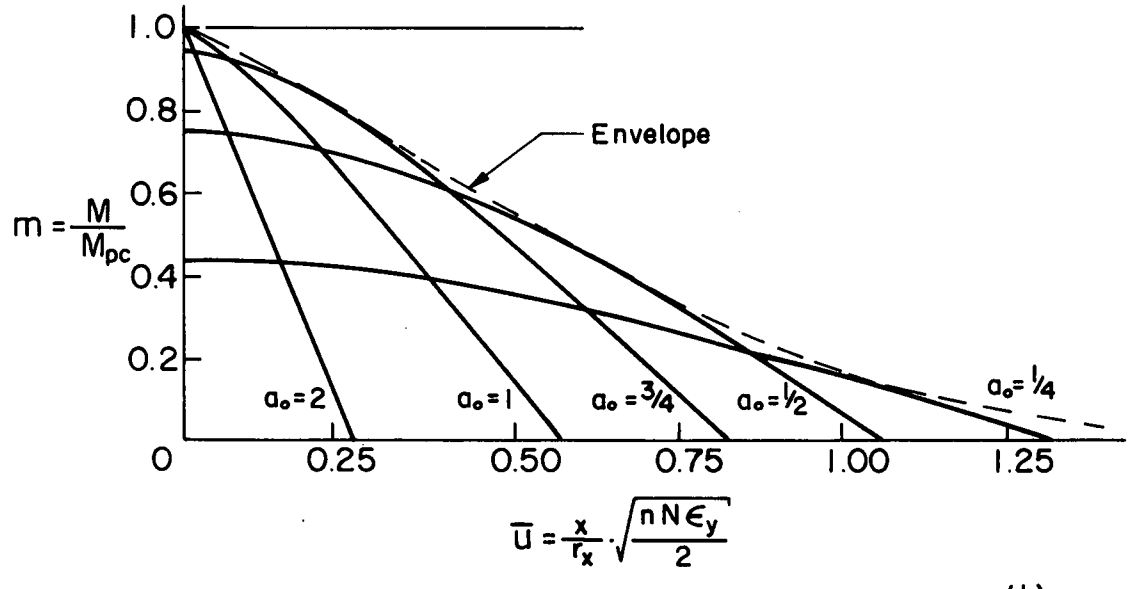

Fig. 5 Column Deflection Curves Plotted To U & $\bar{U}$ Co-ordinates

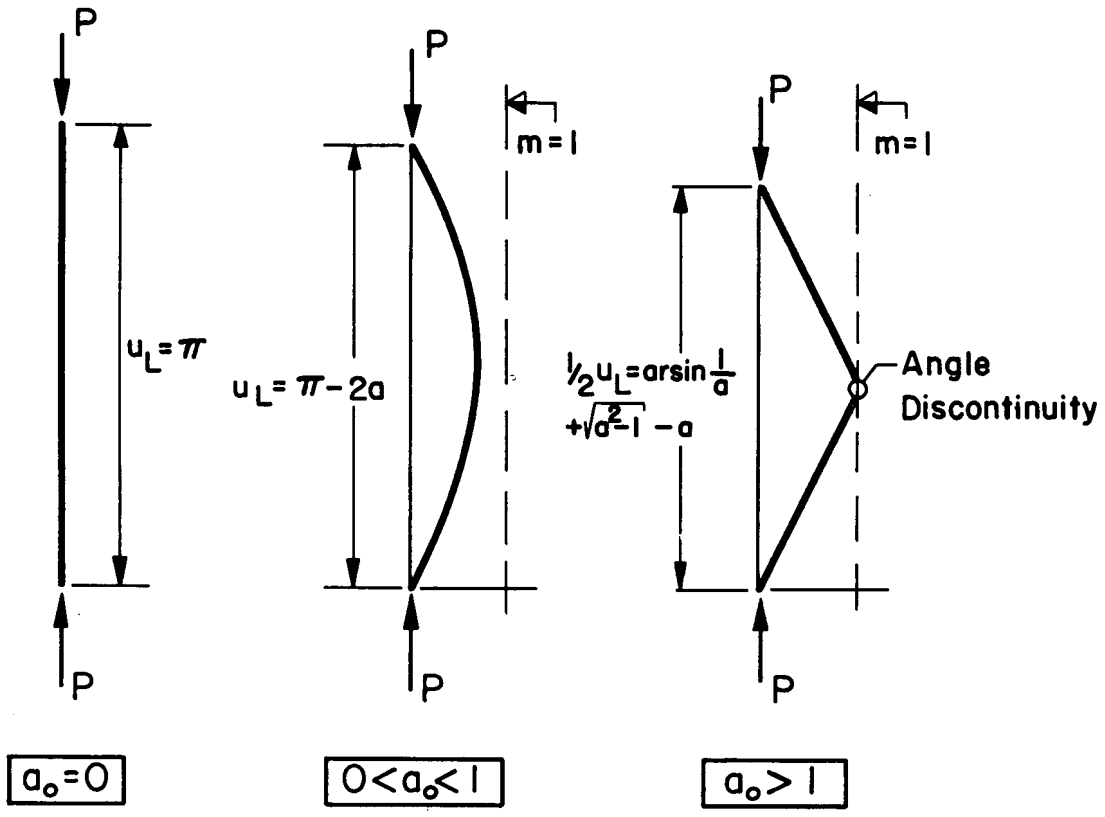

Fig. 6 Diagrammatic Sequence OfColumn Deformation

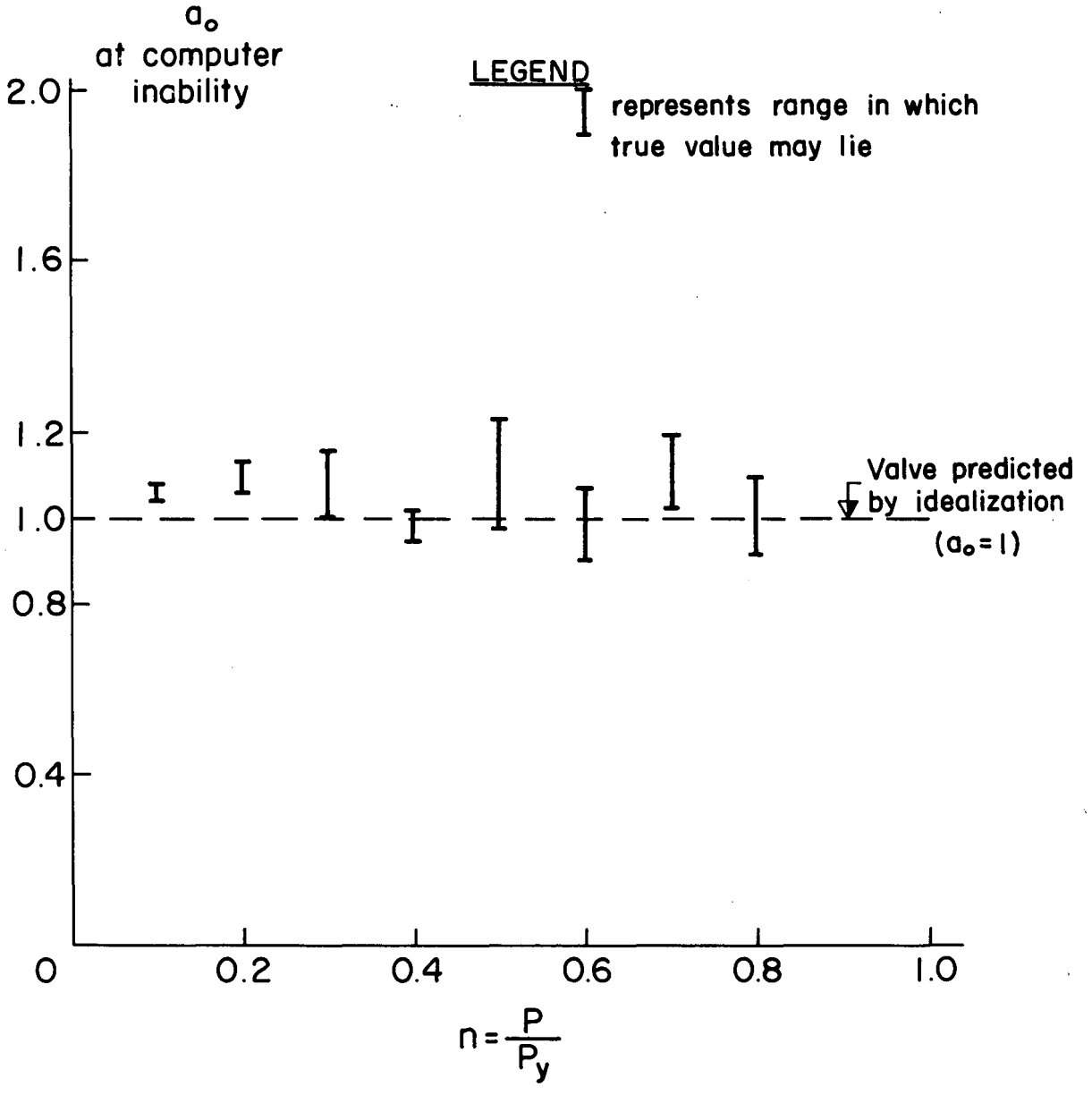

Fig. 7 Comparison Between Hypothetical And Wide Flange Computer Solutions

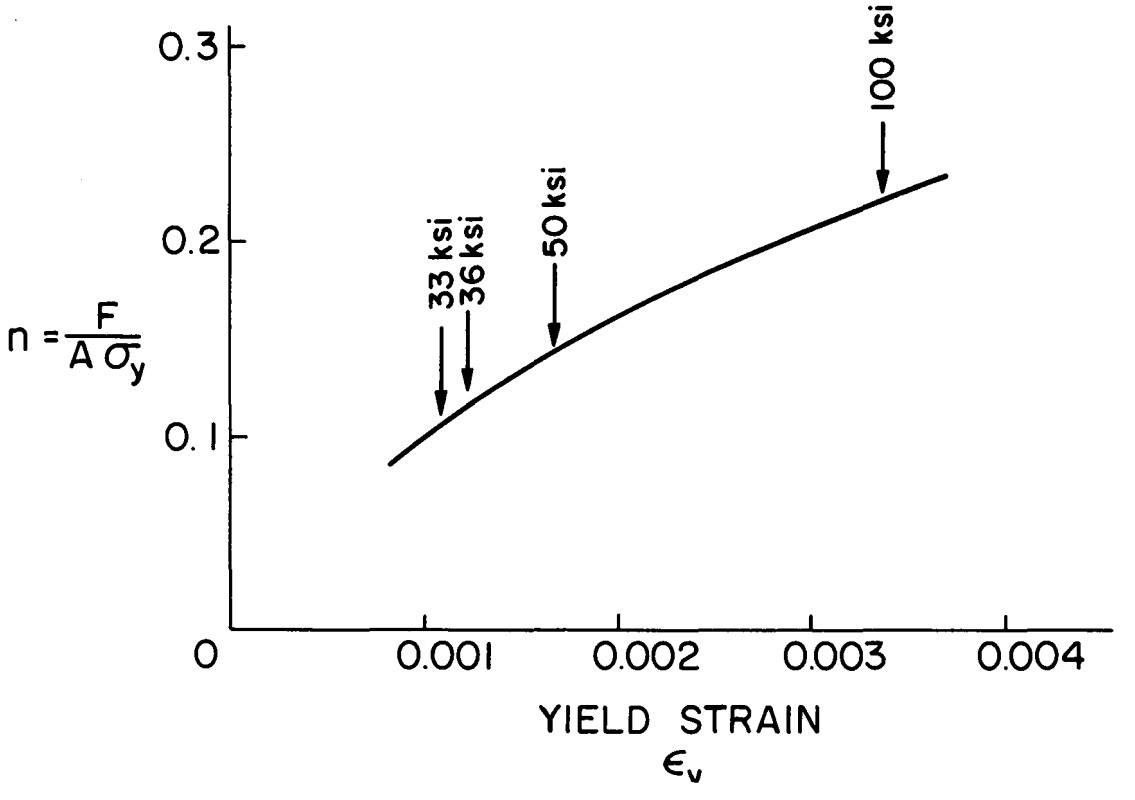

Fig. 8 Critical Load Values For Bending Assumptions

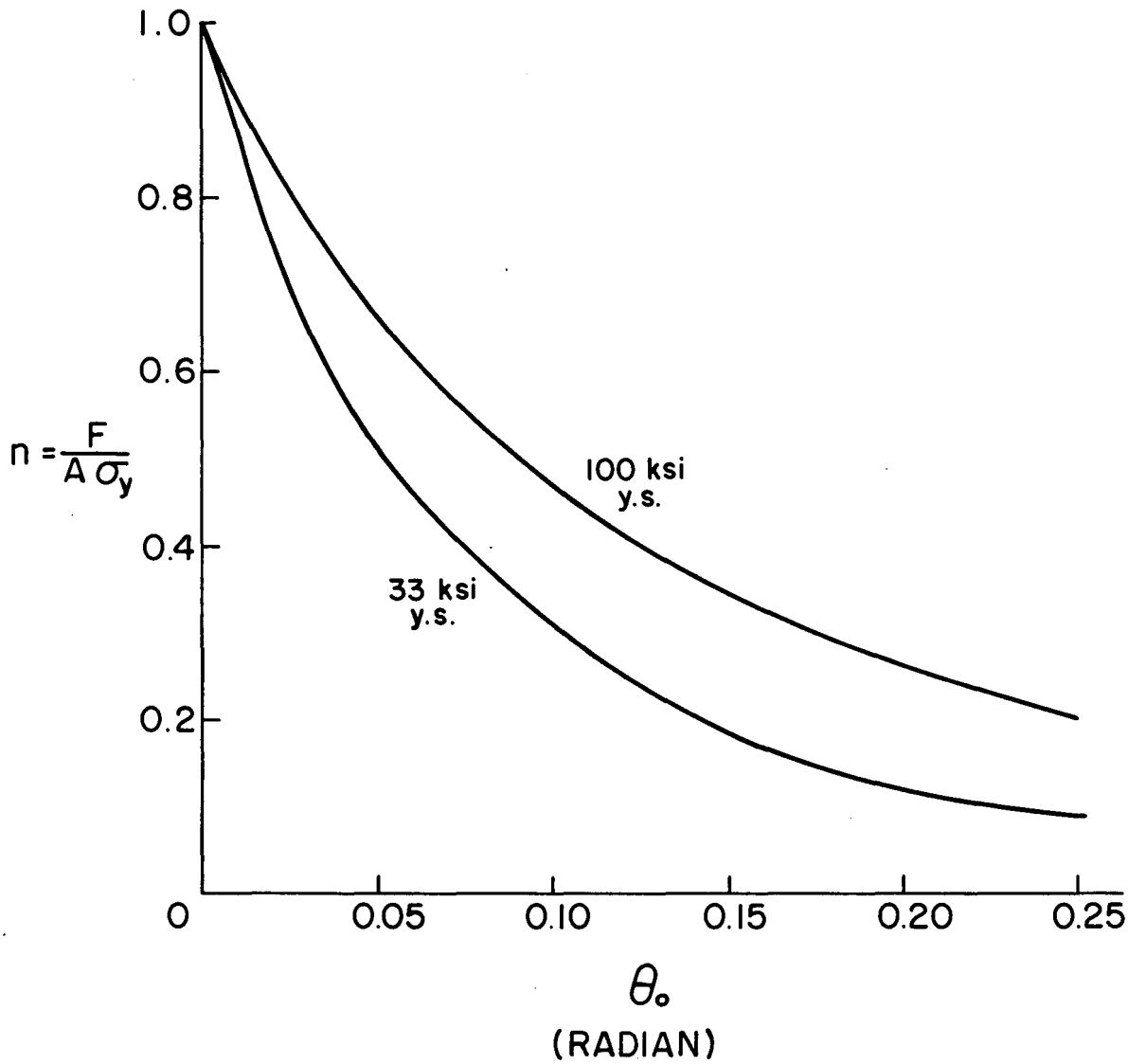

Fig. 9 Values Of θ_o Corresponding To $a_o = 1$

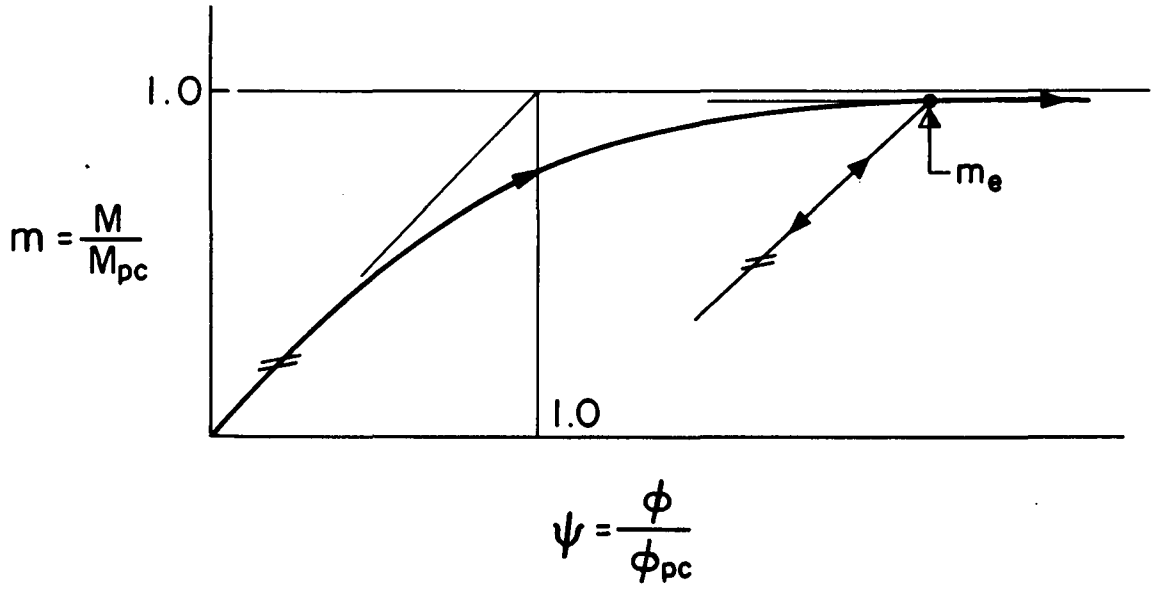

Fig. 10 Moment-Curvature Curve With Unloading

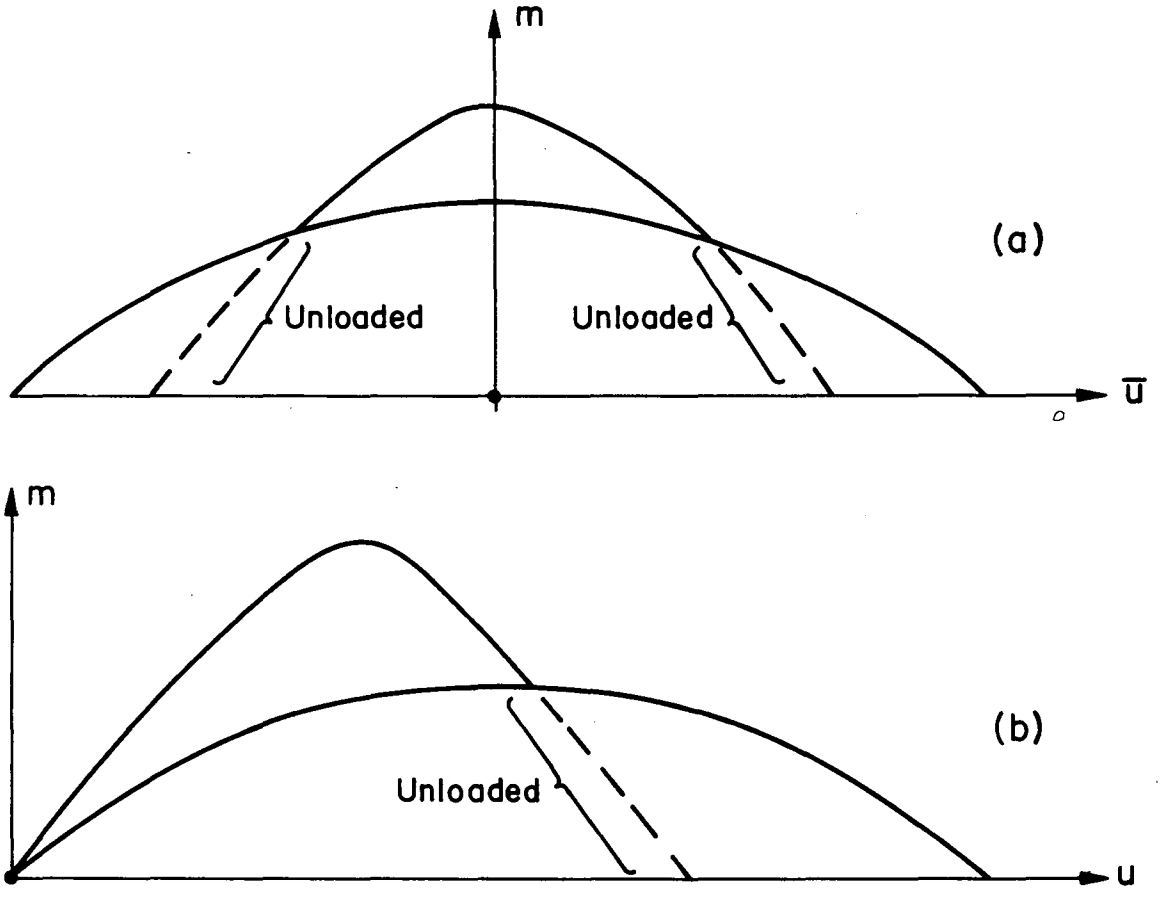

Fig. 11 Illustration of How Axis Location Affects Location Of Unloaded Regions

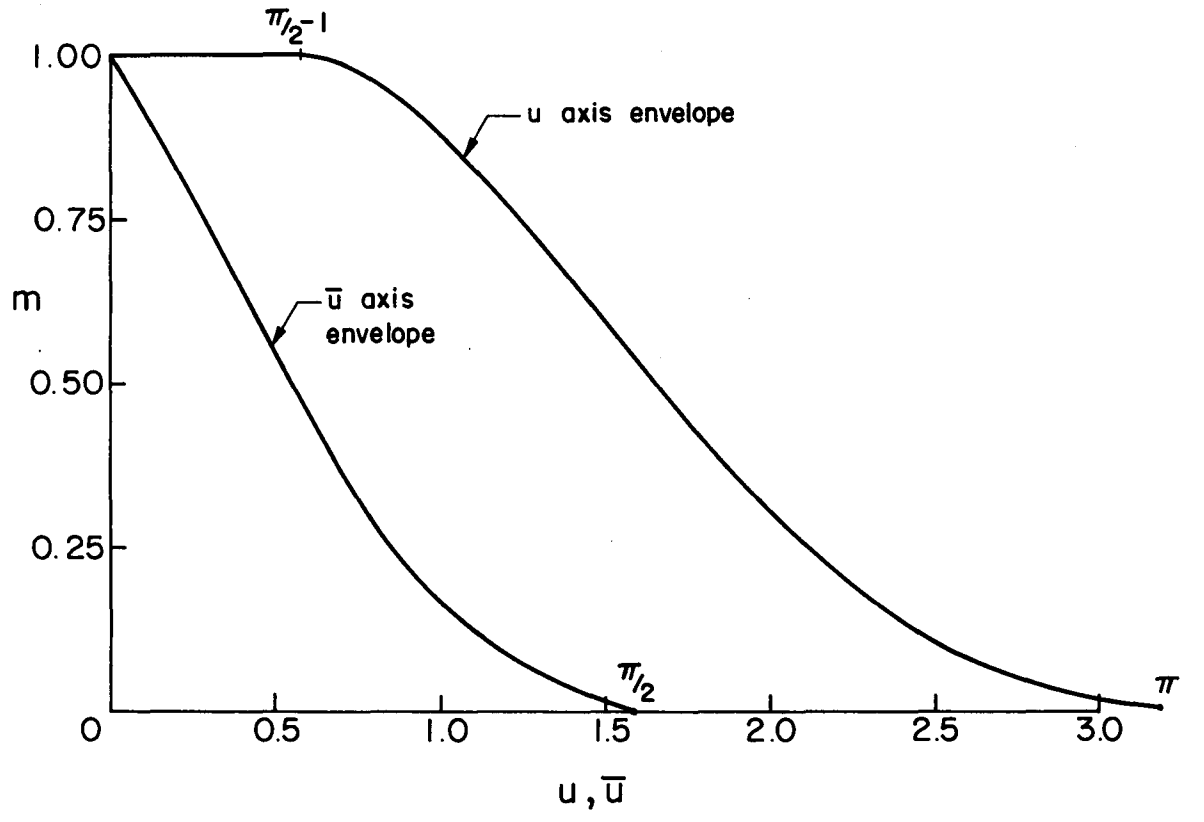

Fig. 12 CDC Envelopes For U & $\bar{U}$ Axes

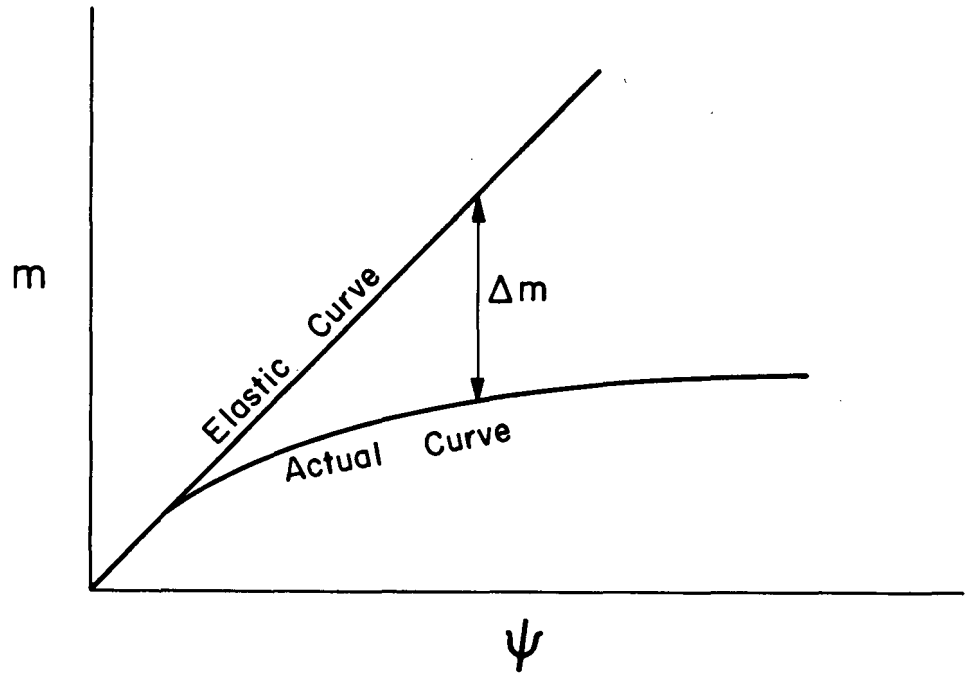

Fig. 13 Definition Of Δm

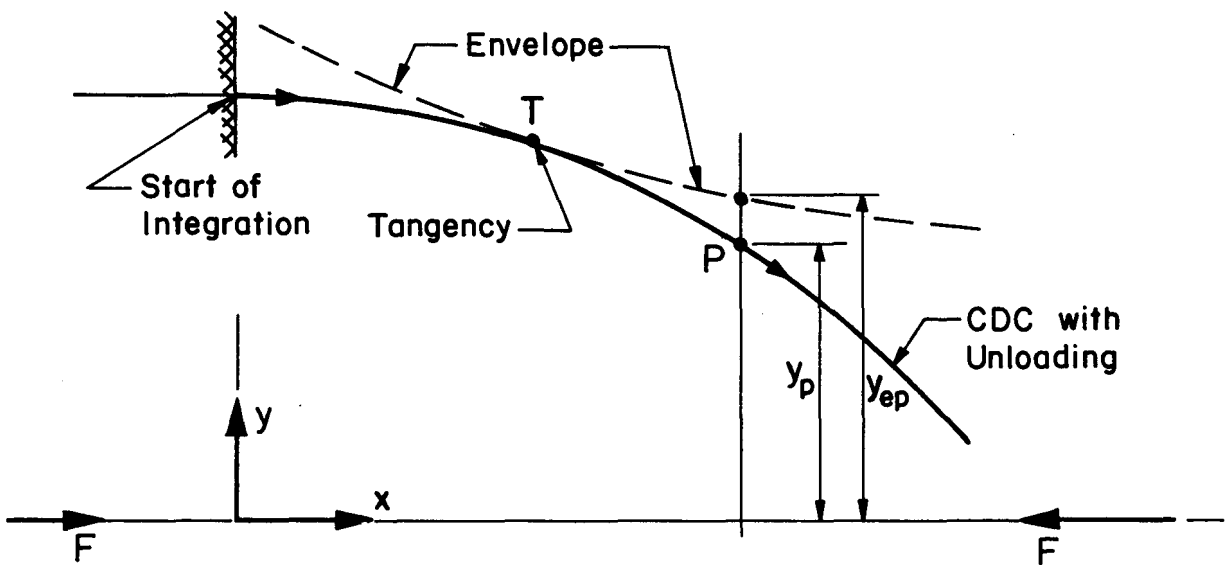

Fig. 14 CDC Considering Unloading

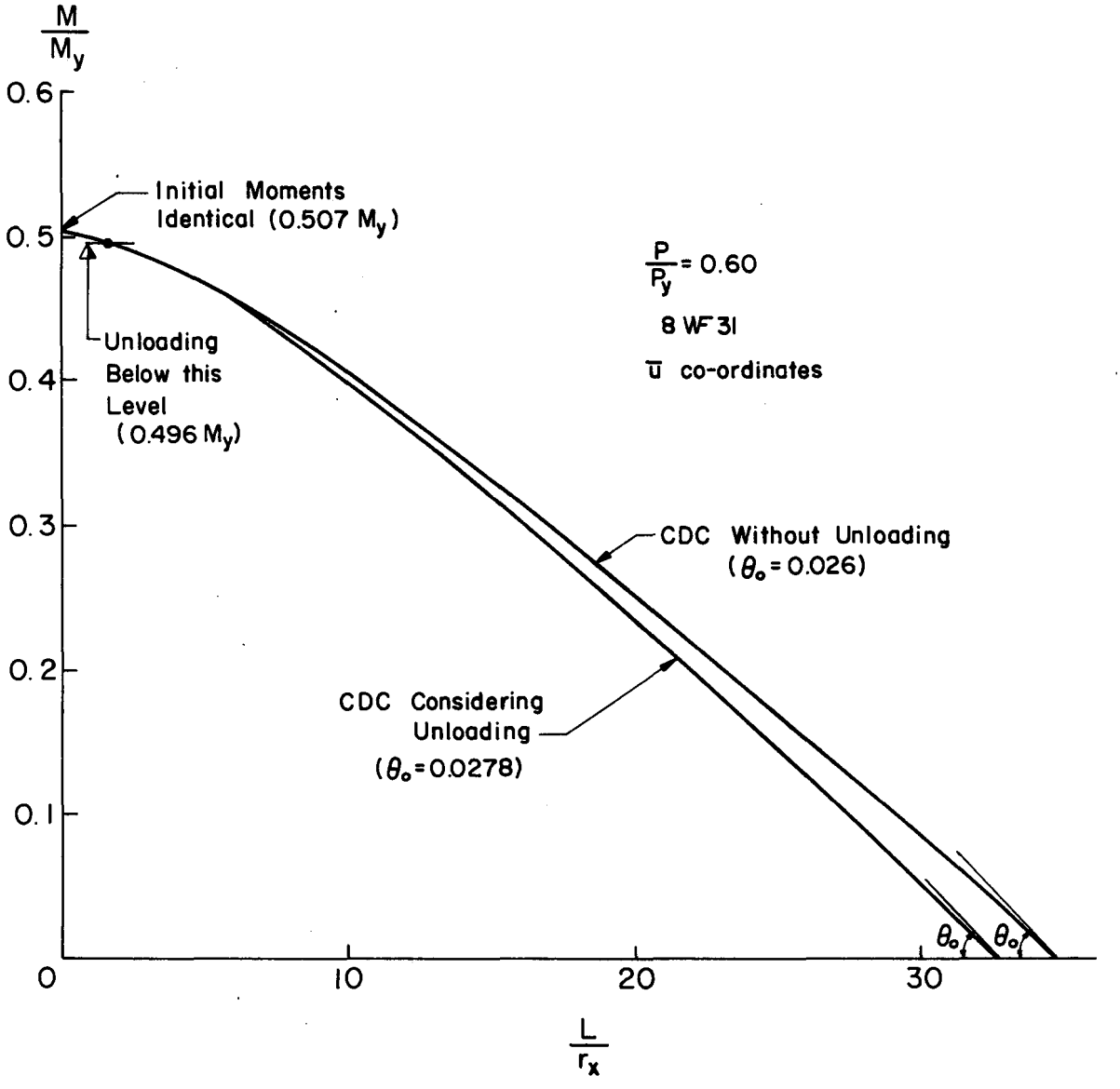

Fig. 15 CDC's With And Without Unloading

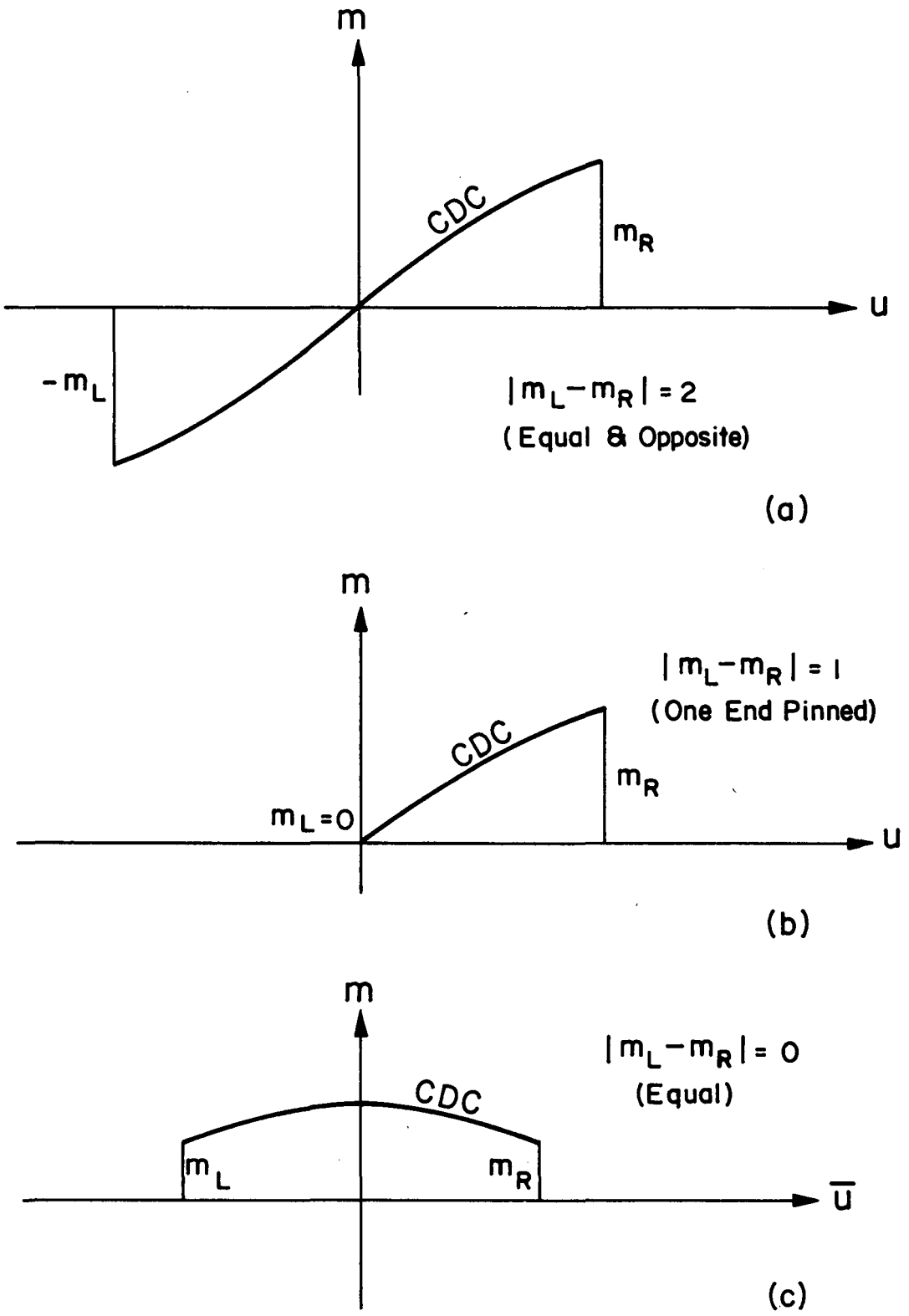

Fig. 16 Beam-Column Representation By CDC Axes

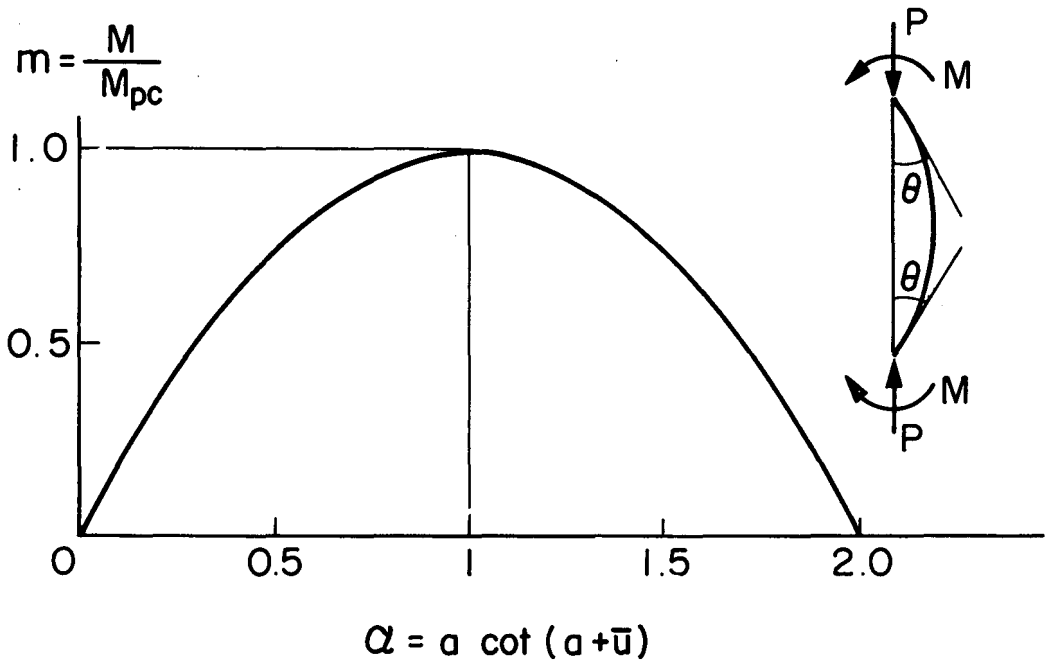

Fig. 17a Parametric Moment-Rotation Curve

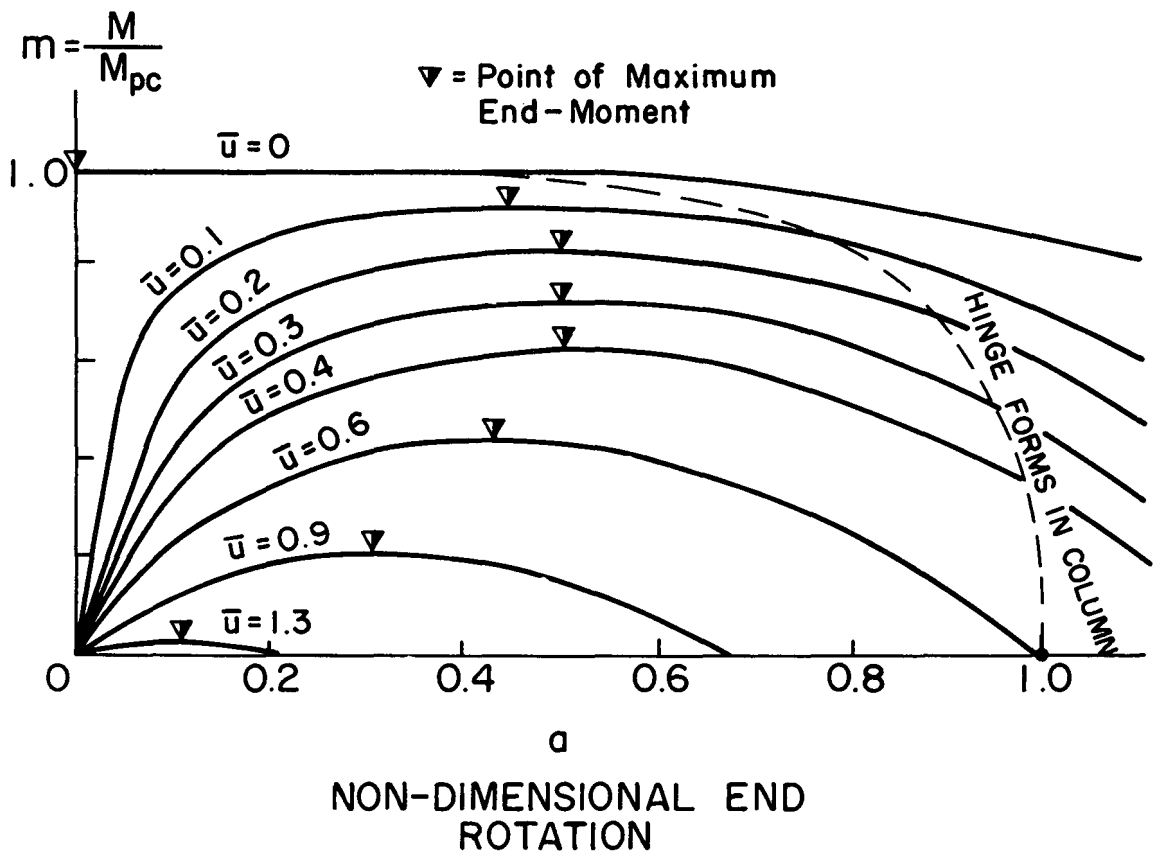

Fig. 17b Moment-Rotation Curves

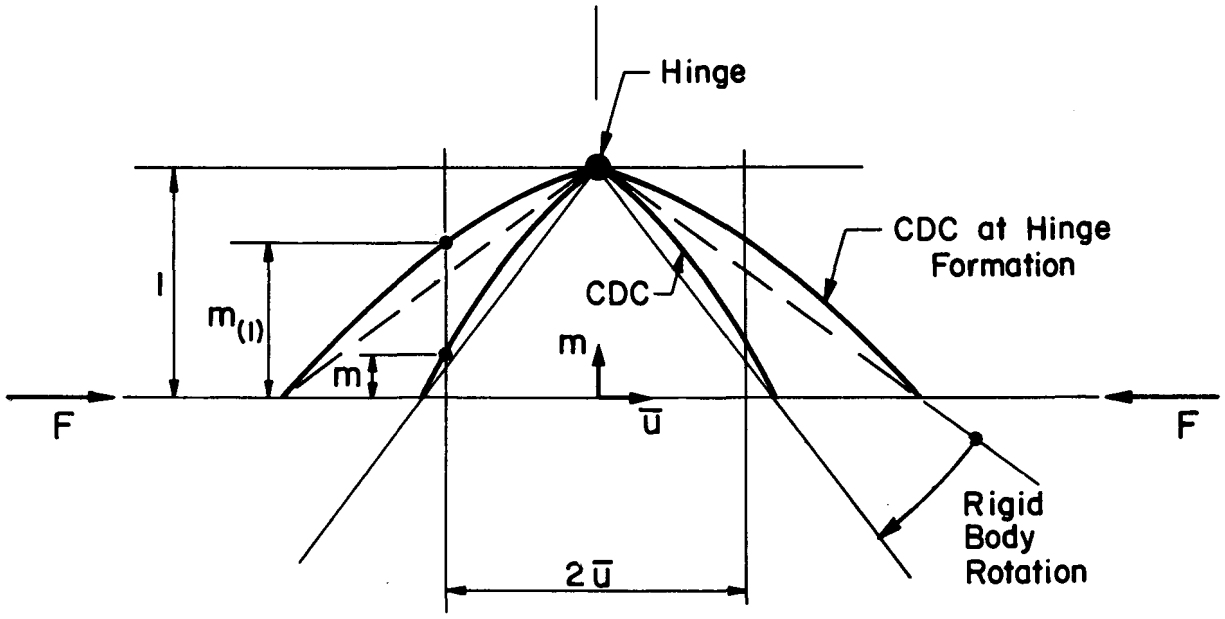

Fig. 18 Post-Hinge Behavior Of Equal End-Moment Case

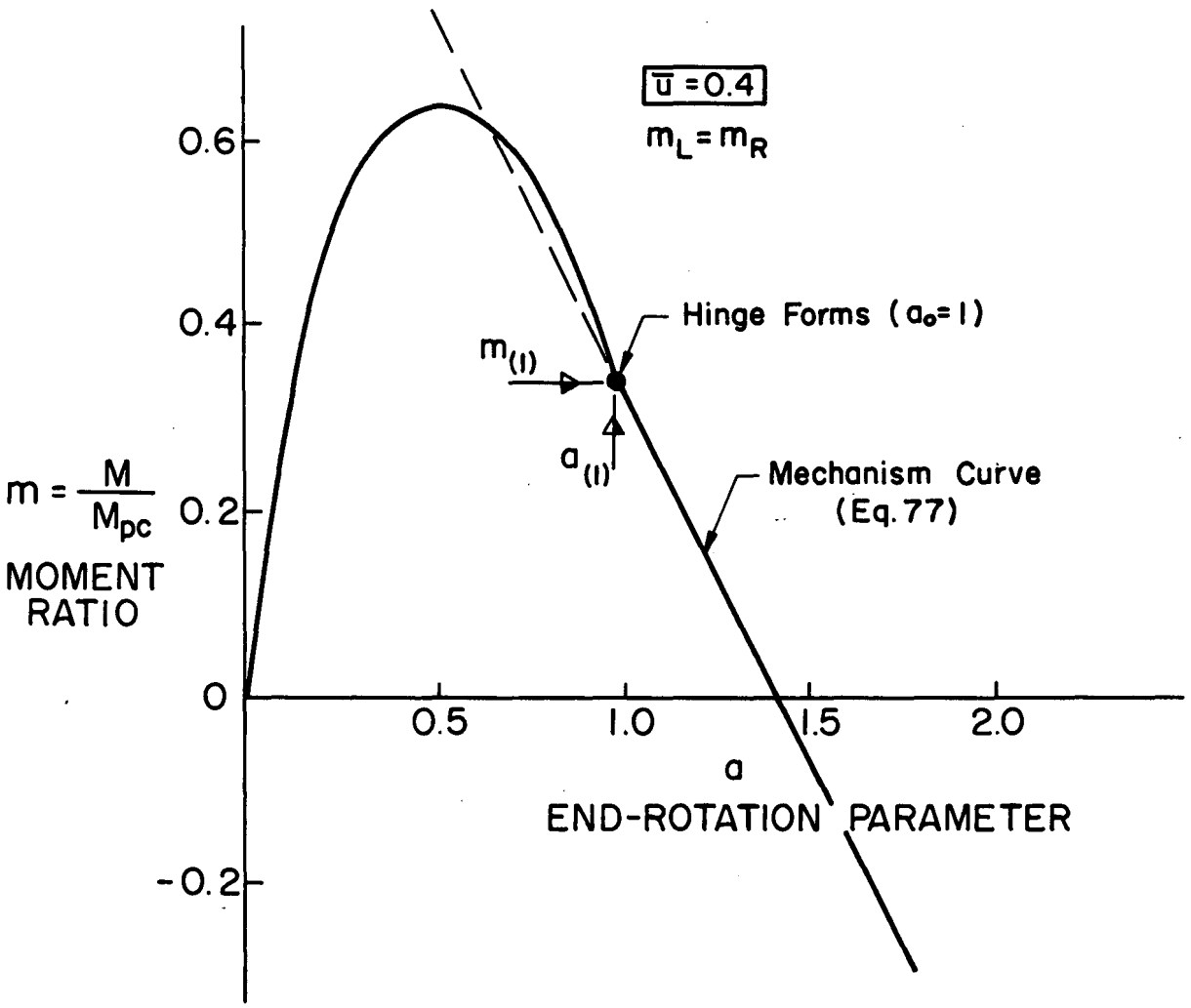

Fig. 19 Post-Hinge Behavior

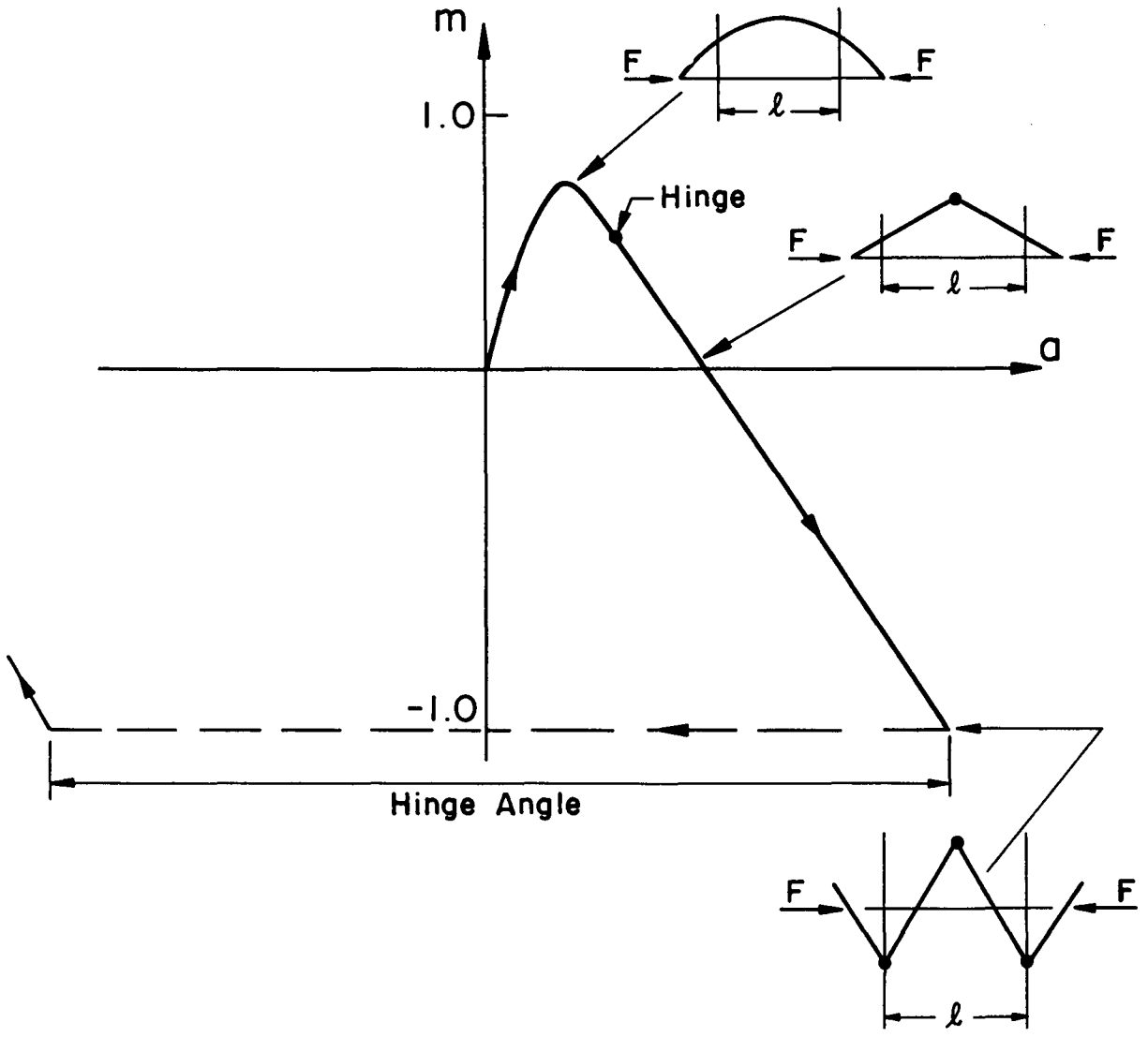

Fig. 20 Behavior At Large Deflections

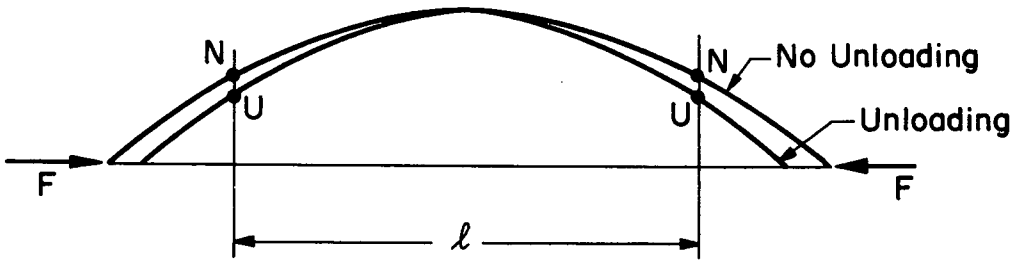

Fig. 21a CDC's With & Without Unloading

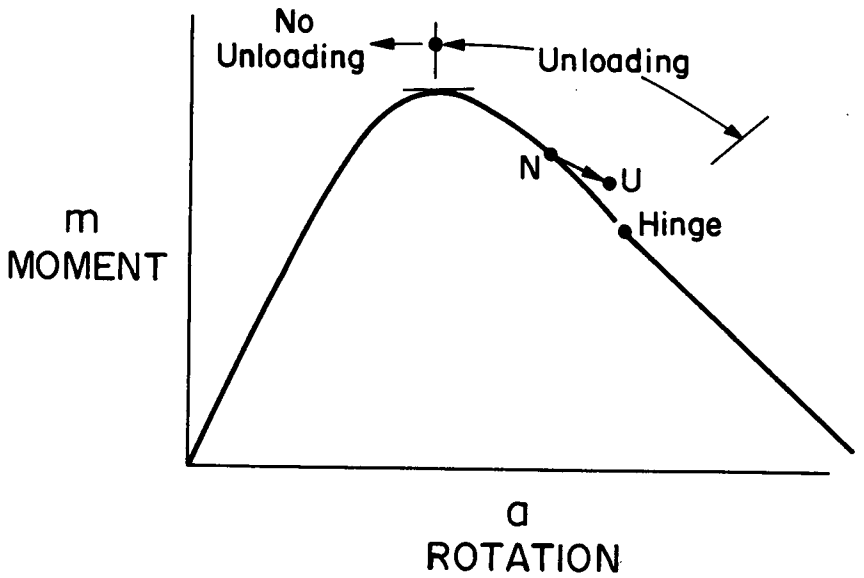

Fig. 21b Moment-Rotation Curve With Unloading

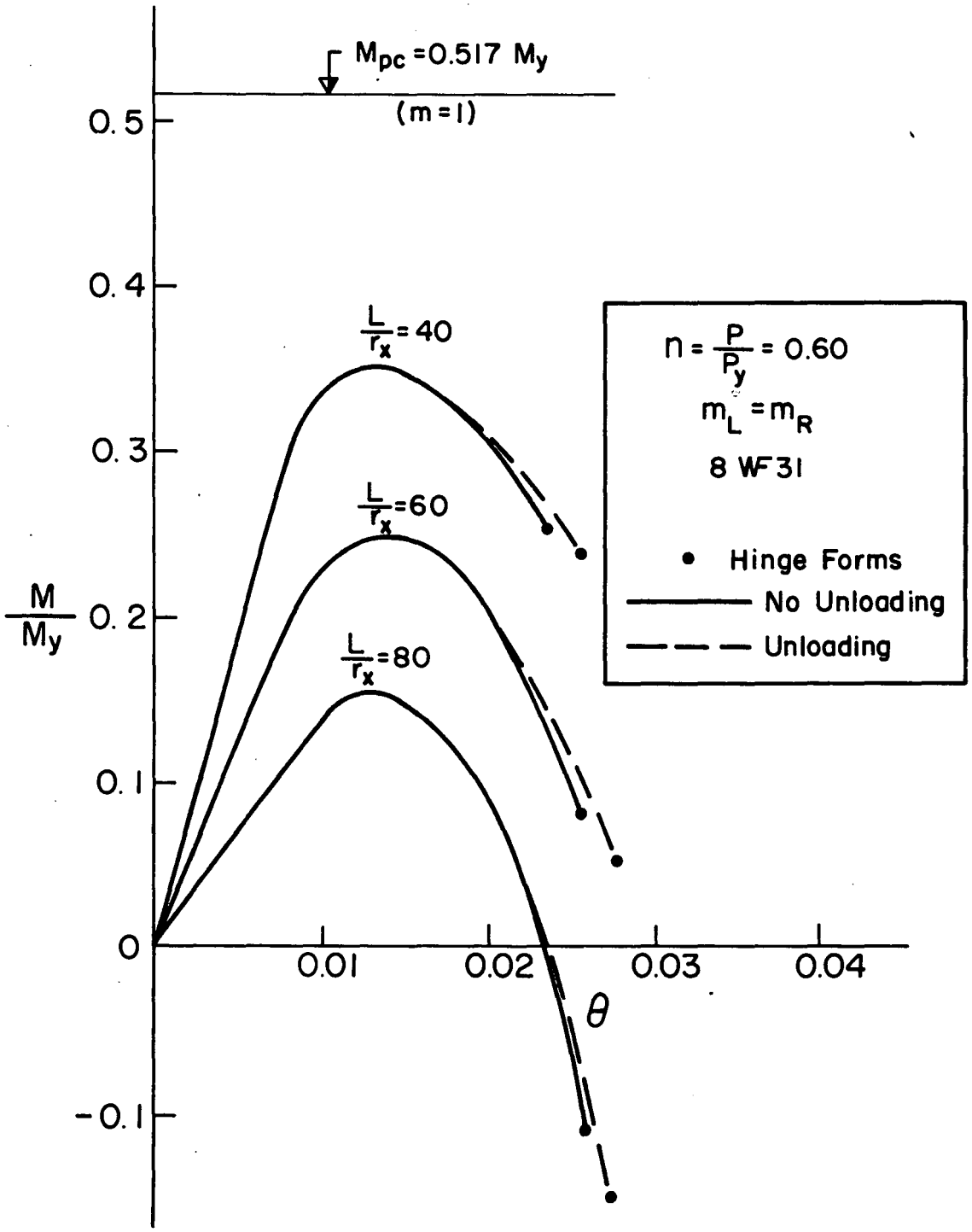

Fig. 22 Beam-Column Curve with Unloading

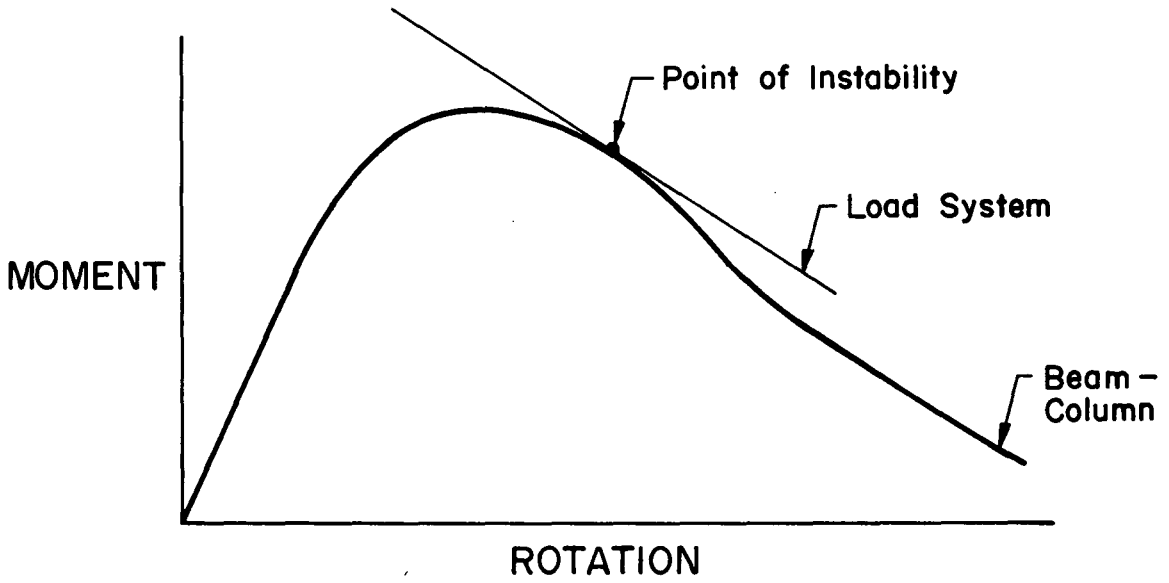

Fig. 23 Beam-Column Instability

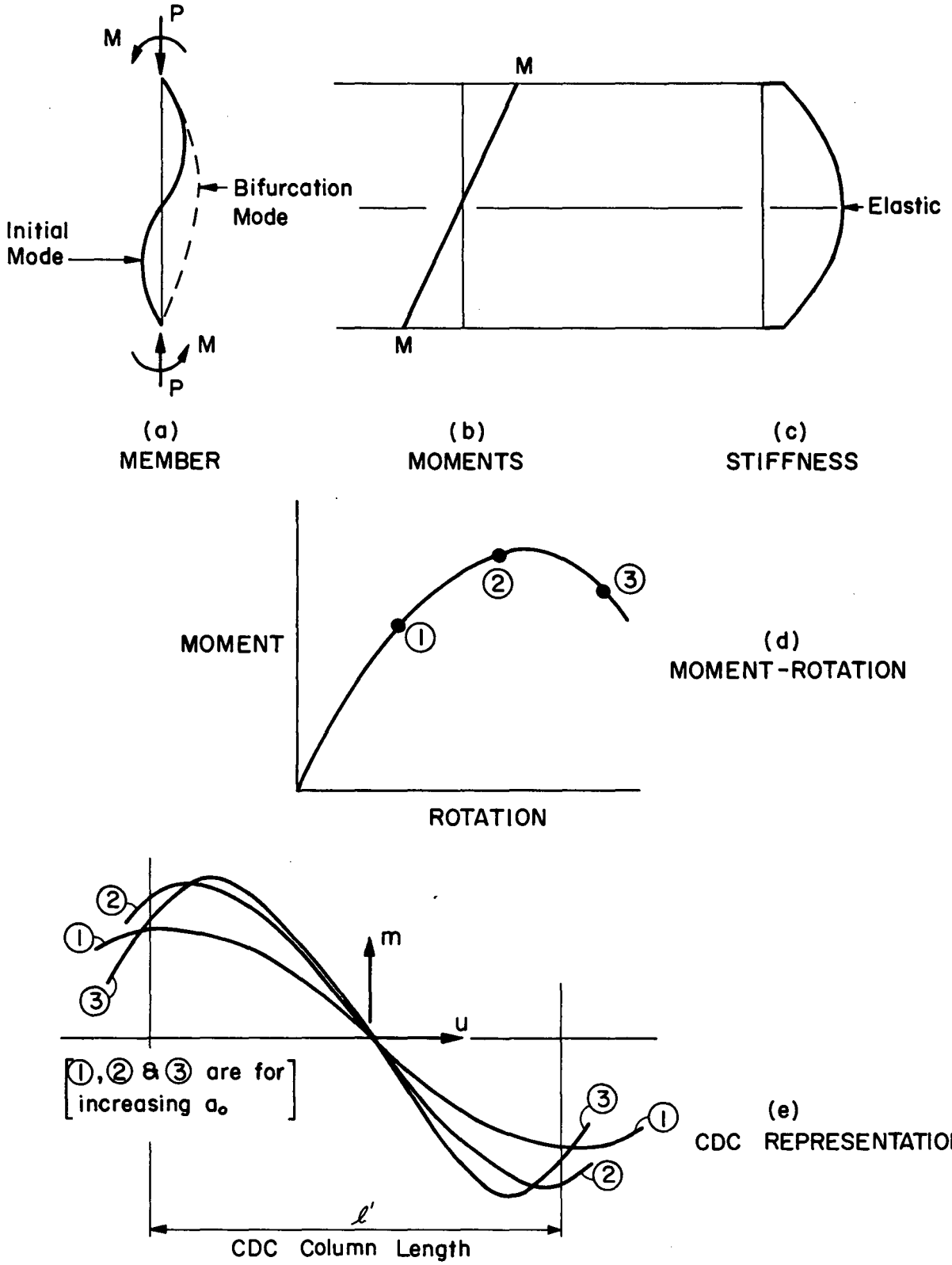

Fig. 24 Unwinding

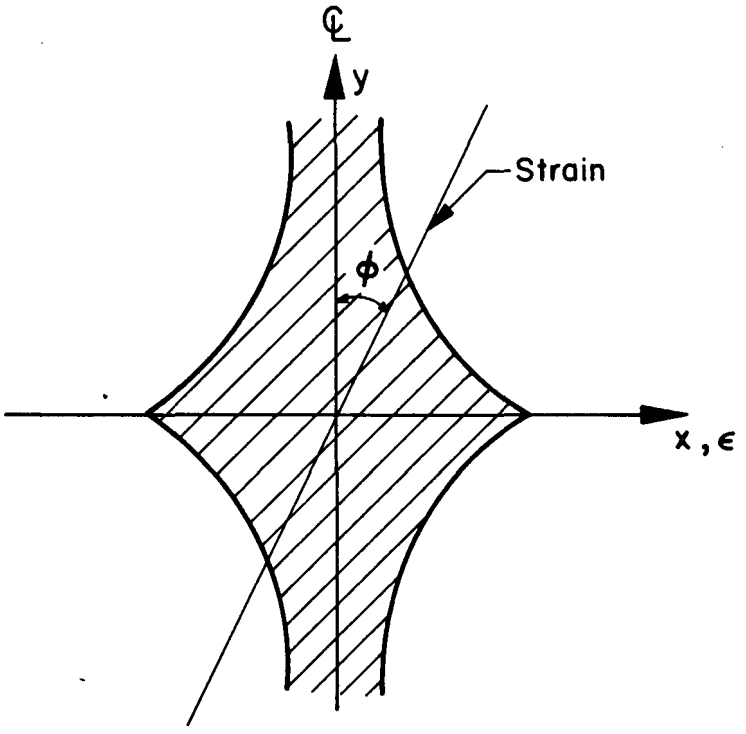

Fig. A1 General Cross-Section

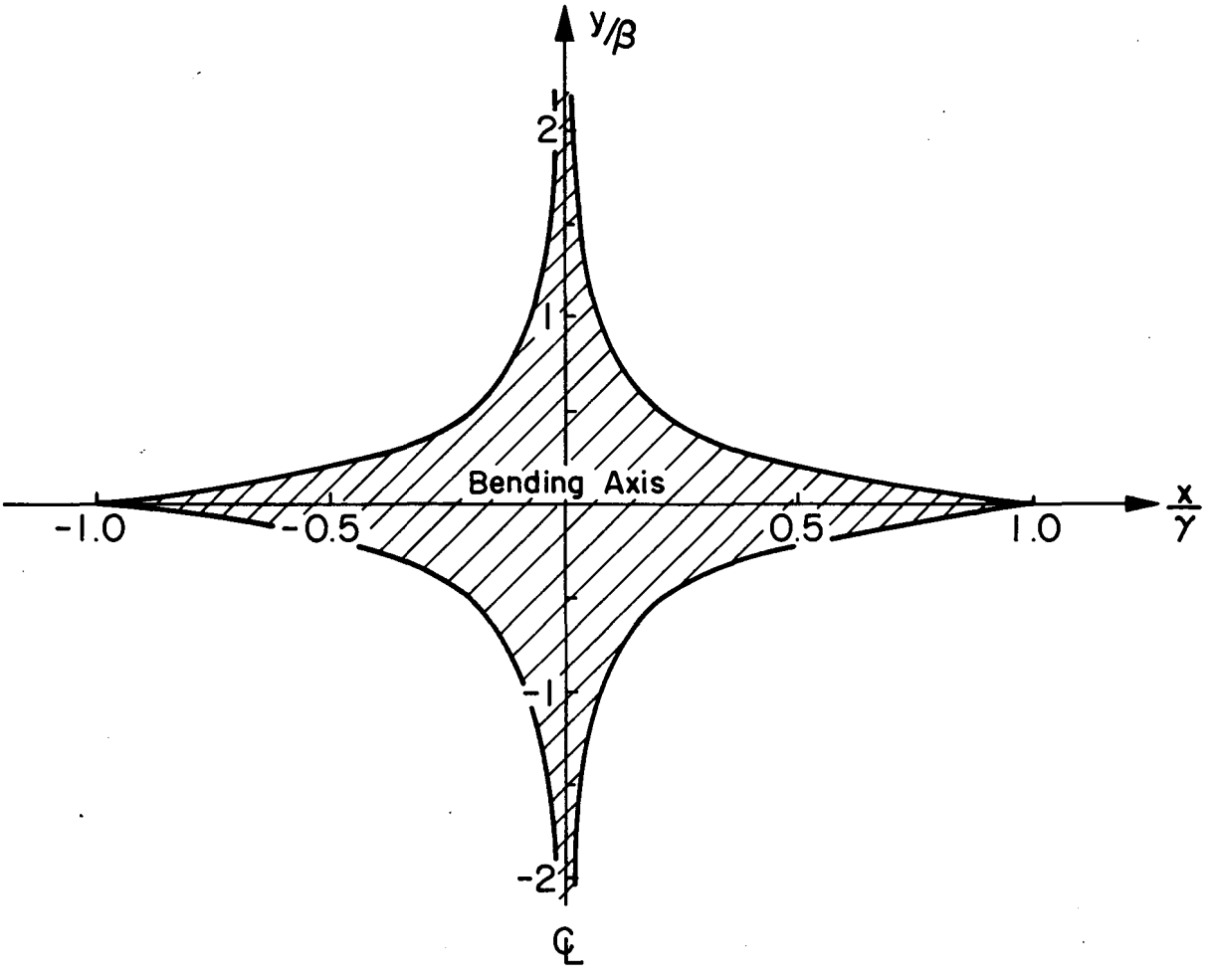

Fig. A2 Section Corresponding To Assumed m-φ Relation

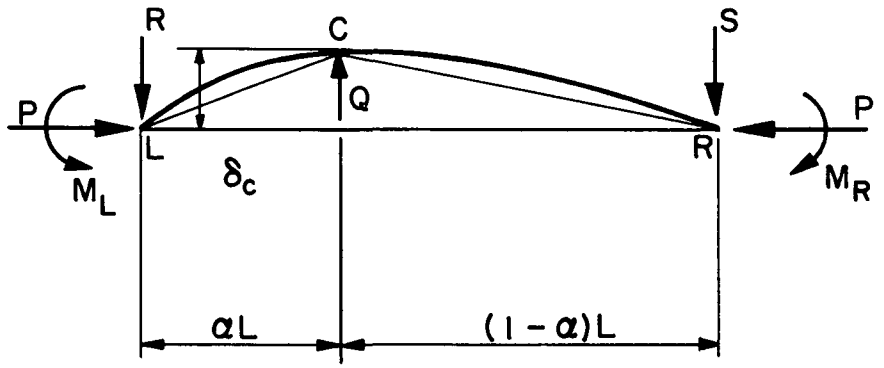

Fig. B1a Laterally Loaded Beam-Column

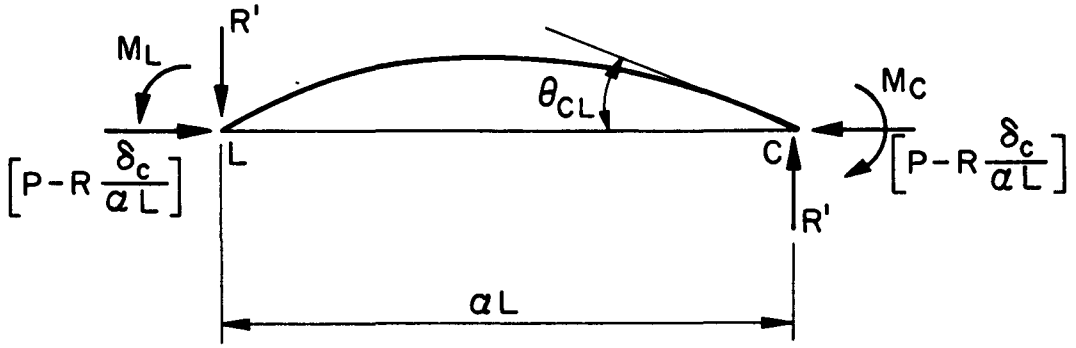

Fig. B1b Left Segment Of Beam-Column

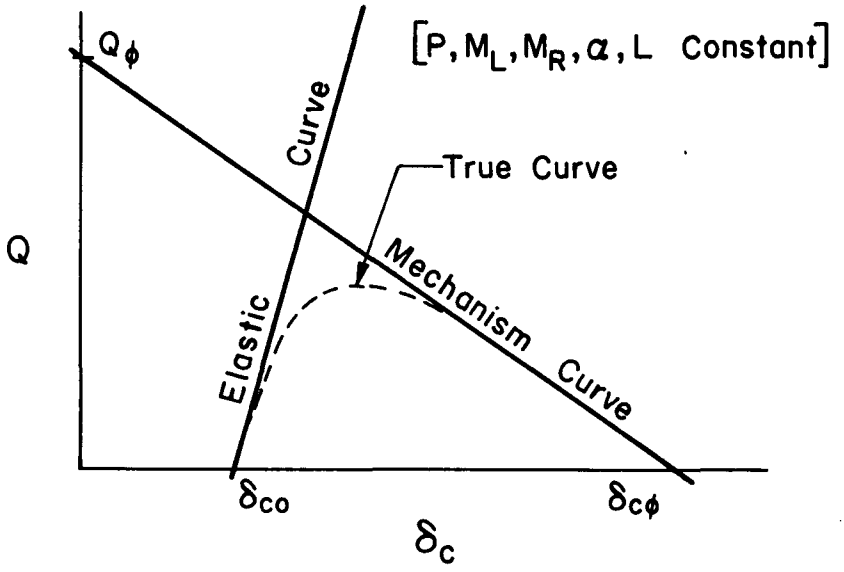

Fig. B2 Graph To Aid In Selection of Q & δ_c Values

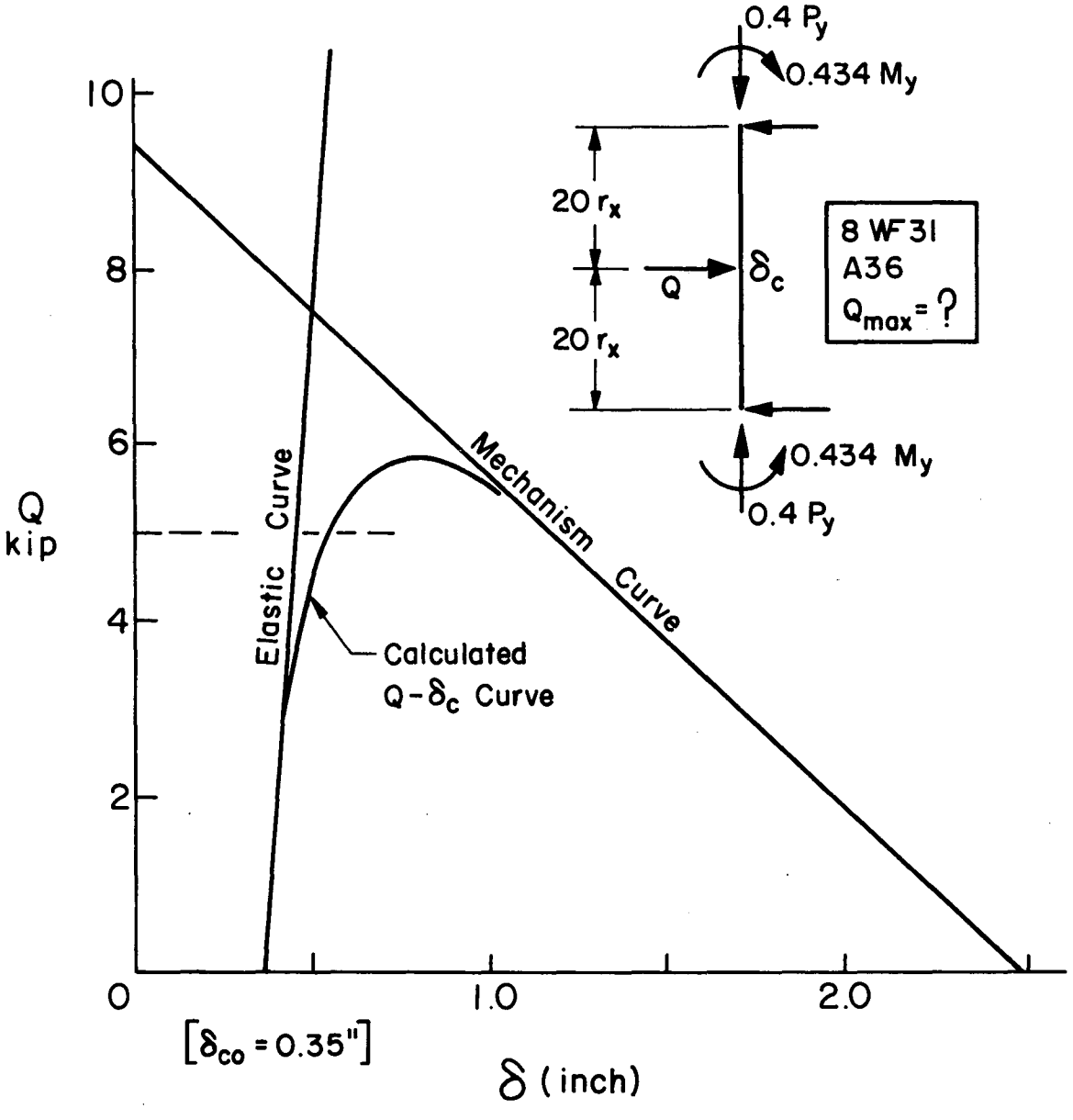

Fig. B3 Illustrative Solution

XII REFERENCES

1. von Karman, T.
   UNTERSUCHUNGEN UBER KNICKFESTIGKEIT
   Mitt. u. Forschungsarb. V.D.I., 81, Berlin, 1910

2. Chwalla, E.
   THEORIE DES AUSSERMITTIG GEDRUCKTEN STABES AUS BAUSTAHL
   Der Stahlbau, 7(21), p. 161-165 (October 1934)
   7(22), p. 173-176 (October 1934)
   7(23), p. 180-184 (November 1934)

3. Chwalla, E.
   DER EINFLUSS DER QUERSCHNITTSFORM AUF DAS TRAGVERMOGEN AUSSERMITTIG GEDRUCKTER BAUSTAHLSTABE
   Der Stahlbau, 8(25), p. 193-197 (December 1935)
   8(26), p. 204-207 (December 1935)

4. Chwalla, E.
   AUSSERMITTIG GEDRUCKTE BAUSTAHLSTABE MIT ELASTISCH EINGESPANNTEN ENDEN UNDER VERSCHIEDEN GROSSEN ANGRIFFSHEBELN
   Der Stahlbau, 10(7), p. 49-52, (March 1937)
   10(8), p. 57-60, (April 1937)

5. Ellis, J.
   PLASTIC BEHAVIOR OF COMPRESSION MEMBERS
   J. Mech and Phys. Solids, 6, p. 282 (1958)

6. Ojalvo, M.
   RESTRAINED COLUMNS
   Proc. ASCE, 86 (EM5), p.1 (October 1960)

7. Neal, B. G. and Mansell, D. S.
   THE EFFECT OF RESTRAINT UPON THE COLLAPSE LOADS OF MILD STEEL TRUSSES
   Int. J. Mech Sci., 5, pp87-97, (Feb 1963)

8. Ros, M. and Brunner, J.
   Proc. 2nd Int. Cong. Appl. Mech, Zurich, p. 368 (1926)

9a. Bijlaard, P., Fisher, G. and Winter, G.
   STRENGTH OF COLUMNS ELASTICALLY RESTRAINED AND ECCENTRICALLY LOADED
   Proc. ASCE, 79 (Sept. 292), (Oct. 1963)

9b. Bijlaard, P.
   BUCKLING OF COLUMNS WITH EQUAL AND UNEQUAL END ECCENTRICITIES AND END ROTATIONS
   Proc. 2nd U.S. Nat. Cong. Appl. Mech. p. 555 (1954)

10. Horne, M. R.
THE ELASTIC-PLASTIC THEORY OF COMPRESSION MEMBERS
J. Mech and Phys. Solids, 4, pp 104-120, (1956)

11. Mansell, D.
DISCUSSION OF REF. 6 "RESTRAINED COLUMNS"
Proc ASCE, 87 (EM1), p. 181, (Feb. 1961)

12. Ojalvo, M. and Fukumoto, Y.
NOMOGRAPHS FOR THE SOLUTION OF BEAM-COLUMN PROBLEMS
Weld.Res.Council Bull, 78, June 1962

13. Hauk, G. and Lee, S-L
STABILITY OF ELASTO-PLASTIC WIDE FLANGE COLUMNS
Proc. ASCE, 89 (ST6), p. 297 (Dec. 1963)

14. Lay, M. and Galambos, T.
DISCUSSION OF REF.13 "STABILITY OF ELASTO-PLASTIC WIDE FLANGE COLUMNS"
Proc. ASCE, 90 (ST-2), p. 419 (April 1964)

15. Lay, M.
THE EXPERIMENTAL BASES FOR PLASTIC DESIGN, (Group 14).
Fritz Engineering Lab. Rep. 297.3 (March 1963)

16. Ojalvo, M.
Discussion of "THE PLASTIC METHOD OF DESIGNING STEEL STRUCTURES" by J. F. Baker
Proc. ASCE, 85 (ST9), p. 89, (Nov. 1959)

17. Paris, P.
LIMIT DESIGN OF COLUMNS
J. Aer. Sci., 21, p. 43 (1954)

18. Hildebrand, F.
ADVANCED CALCULUS FOR ENGINEERS
Prentice-Hall, New York (1949)

19. Levi, V. and Driscoll, G. Jr.
RESPONSE OF COLUMNS TO IN-PLANE LOADING
Fritz Engrg. Lab. Rep. 273.10 (April 63)

20. Galambos, T. and Lay, M.
END-MOMENT END-ROTATION CHARACTERISTICS FOR BEAM-COLUMNS
Fritz Engineering Lab. Rep. 205A.35 (May 1962)

21. Lay, M. and Galambos, T.
TESTS ON BEAM AND COLUMN SUBASSEMBLAGES
Fritz Engrg. Lab. Rep. 278.10 (In preparation)

22. Lay, M.
DISCUSSION OF REF. 7. "THE EFFECT OF RESTRAINT UPON THE COLLAPSE LOADS OF MILD STEEL TRUSSES"
Int. J. Mech Sci., 6 (3), 1964

23. Lay, M.
THE LOAD-DEFORMATION BEHAVIOR OF PLANAR STEEL STRUCTURES
Ph.D. Dissertation, Lehigh Univ. 1964
(Also Fritz Engrg. Lab. Rep. 297.6, 1964)

24. Van Kuren, R. and Galambos, T.
BEAM-COLUMN EXPERIMENTS
Proc. ASCE, 90 (ST-2), p. 223 (April 1964)

25. Ketter, R.
FURTHER STUDIES OF THE STRENGTH OF BEAM-COLUMNS
Proc. ASCE, 87 (ST-6), p. 135 (August 1961)

26. Ojalvo, M.
DISCUSSION OF REF. 25
Proc. ASCE, 87 (ST 8), p. 266 (December 1961)

27. Ketter, R.
CLOSURE TO REF. 25
Proc. ASCE, 88 (ST 3), p. 319 (June 1962)

28. Tall, L.
STRUCTURAL STEEL DESIGN, Ch. 9
Ronald Press, New York, 1964